

THE FUNCTION OF PHOSPHATIDYLINOSITOL 4-KINASE III-BETA IN  
*TRYPANOSOMA BRUCEI*

APPROVED BY SUPERVISORY COMMITTEE

---

Margaret Phillips, Ph.D.

---

Joe Albanesi, Ph.D.

---

Melanie Cobb, Ph.D.

---

Helen Yin, Ph.D.

## DEDICATION

To my family for their patience and encouragement throughout my education and to  
Vince and Jellybean, for their love and support.

THE FUNCTION OF PHOSPHATIDYLINOSITOL 4-KINASE III-BETA IN  
*TRYPANOSOMA BRUCEI*

by

MELISSA JEANE RODGERS

DISSERTATION

Presented to the Faculty of the Graduate School of Biomedical Sciences

The University of Texas Southwestern Medical Center at Dallas

In Partial Fulfillment of the Requirements

For the Degree of

DOCTOR OF PHILOSOPHY

The University of Texas Southwestern Medical Center at Dallas

Dallas, Texas

December, 2006

Copyright

by

MELISSA JEANE RODGERS, 2006

All Rights Reserved

THE FUNCTION OF PHOSPHATIDYLINOSITOL 4-KINASE III-BETA IN  
*TRYPANOSOMA BRUCEI*

MELISSA JEANE RODGERS, Ph.D.

The University of Texas Southwestern Medical Center at Dallas, 2006

MENTOR: MARGARET A. PHILLIPS, Ph.D.

Phosphatidylinositol 4-kinase phosphorylates phosphatidylinositol at the D4 position resulting in phosphatidylinositol 4-monophosphate. Subsequent phosphorylation events result in a group of molecules known as phosphoinositides. These molecules are important in signal transduction, endocytosis, exocytosis, and protein trafficking. Two phosphatidylinositol 4-kinases are found in *Trypanosoma brucei*. We have cloned the gene encoding the Type III phosphatidylinositol 4-kinase Beta (TbPI4KIII- $\beta$ ) in *Trypanosoma brucei*. The protein was exogenously expressed in COS-7 cells and assayed for phosphatidylinositol kinase activity. The expressed protein migrated on

SDS-PAGE near the predicted molecular weight of 66 kDa and phosphorylates phosphatidylinositol. Depletion of TbPI4KIII- $\beta$  in procyclic *T. brucei* by RNAi results in inhibition of cell growth and a distorted cellular morphology. Immunofluorescence studies revealed a distorted Golgi apparatus and mislocalization of lysosomal and flagellar pocket proteins. Ultrastructural analysis reveals internal accumulation of a heterogeneous population of vesicles, abnormal positioning of organelles and a loss of cell polarity. Scanning EM reveals a twisted morphology most likely due to an alteration in the microtubule cytoskeleton. Dividing TbPI4KIII- $\beta$  RNAi trypanosomes often exhibited a detached daughter flagellum and lacked a cleavage furrow, suggesting a defect in cell division and/or cytokinesis. Cell cycle analysis confirmed that cells depleted of TbPI4KIII- $\beta$  have a post-mitotic cytokinesis block. In summary, TbPI4KIII- $\beta$  is an essential protein in procyclic *T. brucei*, required for maintenance of Golgi structure, protein trafficking, normal cellular shape and cytokinesis.

## TABLE OF CONTENTS

Title-fly .....	i
Dedication .....	ii
Title page .....	iii
Copyright .....	iv
Abstract .....	v
Table of contents .....	vii
List of figures .....	xiii
List of tables .....	xv
List of abbreviations .....	xvi
<b>Chapter 1</b>	
Introduction .....	1
A. <i>Trypanosoma brucei</i> .....	1
1. Overview .....	1
2. African Trypanosomiasis .....	2
3. Biology .....	3
B. Phosphoinositides .....	4
C. Phosphatidylinositol 4-Kinase.....	5
1. Overveiw .....	5
2. Phosphatidylinositol 4-kinase Isoforms .....	6
3. Cellular Functions of Phosphatidylinositol 4-kinase Isoforms.....	7
D. Phosphoinositides in <i>T. brucei</i> .....	9

## **Chapter 2**

Identification and Characterization of Phosphatidylinositol 4-kinase III-Beta.....	14
A. Introduction.....	14
B. Materials and Methods .....	15
1. Cell Culture .....	15
2. Lysate Preparation.....	15
3. In Vitro Kinase Assays.....	16
4. RNA isolation and Northern Blot Analysis.....	17
5. Cloning and Expression.....	17
6. Immunoprecipitation .....	18
7. Immune Complex Kinase Assays.....	19
C. Results .....	19
1. Inhibitor Profile of PCF Lysates.....	19
2. Transcript Levels.....	20
3. Sequence Analysis.....	20
4. Protein Expression and Characterization.....	21
D. Discussion .....	22

## **Chapter 3**

Generation of TbPI4KIII- $\beta$ RNAi Cell Line.....	32
A. Introduction.....	32
B. Materials and Methods.....	33
1. Cell Culture and Transfection .....	33



2. Plasmid construction .....	33
3. RNA Isolation and Northern Blot Analysis.....	34
4. Growth Curves .....	35
5. Inositol Labeling.....	35
C. Results and Discussion.....	35
1. TbPI4KIII- $\beta$ RNAi Cell Line .....	35
2. Depletion of TbPI4KIII- $\beta$ Causes a Defect in Growth.....	36
3. Depletion of TbPI4KIII- $\beta$ Results in a Decrease in PI4P Levels.....	37
<b>Chapter 4</b>	
TbPI4KIII- $\beta$ is required for Normal Morphology in Procyclic <i>T. brucei</i> .....	43
A. Introduction.....	43
B. Materials and Methods .....	44
1. Cell Culture .....	44
2. Immunofluorescence Microscopy and Phenotype Quantitation.....	44
2. Transmission Electron Microscopy.....	45
3. Scanning Electron Microscopy.....	45
C. Results .....	45
1. DIC Images of the Phenotype.....	45
2. Ultrastructural Analysis.....	46
3. Scanning Electron Microscopy.....	47
4. Examination of Abnormal Surface Structure .....	47
D. Discussion .....	48

## Chapter 5

TbPI4KIII- $\beta$ is Required for Normal Golgi Structure and Function .....	57
A. Introduction .....	57
B. Materials and Methods .....	58
1. Cell Culture .....	58
2. Immunofluorescence Microscopy .....	58
3. Transmission Electron Microscopy .....	60
C. Results .....	60
1. TbPI4KIII- $\beta$ is Required for the Correct Localization of Protein Markers .....	60
D. Discussion .....	62

## Chapter 6

TbPI4KIII- $\beta$ is Required for Cytokinesis in Procyclic Form <i>T. brucei</i> .....	69
A. Introduction .....	69
B. Materials and Methods .....	70
1. Cell Culture .....	70
2. Immunofluorescence Microscopy .....	71
3. Analysis of DNA Content .....	71
4. Scanning Electron Microscopy .....	72
C. Results .....	72
1. Effect of TbPI4KIII- $\beta$ Depletion on Cell Cycle Progression in Procyclic Form <i>T. brucei</i> .....	72
2. Effect of TbPI4KIII- $\beta$ Depletion on Kinetoplast and Nuclear Segregation .....	73

3. Dividing TbPI4KIII- $\beta$ Depleted Cells Lack a Cleavage Furrow.....	74
D. Discussion .....	75
<b>Chapter 7</b>	
Conclusion and Future Directions .....	83

#### PRIOR PUBLICATIONS

Rodgers, M.J., Albanesi, J.P., Phillips, M.A. (2007) The Function of Phosphatidylinositol 4-Kinase III-Beta in *Trypanosoma brucei*. In preparation

## LIST OF FIGURES

Figure 1.1. Phosphoinositide Cycle .....	10
Figure 1.2. Phosphatidylinositol 4-kinase reaction .....	11
Figure 1.3. Domain structure of phosphatidylinositol 4-kinase isoforms .....	13
Figure 2.1. Endogenous phosphatidylinositol kinase activity .....	24
Figure 2.2. Northern blot analysis .....	25
Figure 2.3. The nucleotide and translated amino acid sequence of the full-length <i>T. brucei</i> PI4KIII- $\beta$ .....	26
Figure 2.4. Domain structure of TbPI4KIII- $\beta$ and MUSCLE alignments .....	28
Figure 2.5. Western blot of immunoprecipitated Flag-tagged recombinant TbPI4KIII- $\beta$ .....	30
Figure 2.6. Immune complex kinase assay of Flag-tagged recombinant TbPI4KIII- $\beta$ ....	31
Figure 3.1. Stem-loop vector construct .....	39
Figure 3.2. Northern blot analysis of TbPI4KIII- $\beta$ .....	40
Figure 3.3. Effect of TbPI4KIII- $\beta$ depletion on growth .....	41
Figure 3.4. Effect of TbPI4KIII- $\beta$ depletion on phosphatidylinositol monophosphate levels .....	42
Figure 4.1. TbPI4KIII- $\beta$ is required for normal morphology in procyclic <i>T. brucei</i> .....	51
Figure 4.2. Frequency of phenotypes in induced cultures .....	52
Figure 4.3. Ultrastructural analysis of TbPI4KIII- $\beta$ depleted cells .....	53
Figure 4.4. Cells depleted of TbPI4KIII- $\beta$ have an abnormal twisted shape .....	55
Figure 4.5. Cells depleted of TbPI4KIII- $\beta$ eventually collapse .....	56
Figure 5.1. Depletion of TbPI4KIII- $\beta$ does not affect the ER .....	65

Figure 5.2. Abnormal localization of protein markers for the Golgi, lysosome and flagellar pocket in cells depleted of TbPI4KIII-β.....	66
Figure 5.3. Abnormal localization of the lysosomal marker trypanopain in cells depleted of TbPI4KIII-β.....	67
Figure 6.1. Procyclic <i>T. brucei</i> cell cycle .....	78
Figure 6.2. Cell cycle analysis of procyclic form TbPI4KIII-β RNAi cells .....	79
Figure 6.3. Analysis of morphological cell cycle events in procyclic form TbPI4KIII-β RNAi cells.....	80
Figure 6.4. Dividing TbPI4KIII-β depleted cells lack a cleavage furrow.....	81

## LIST OF TABLES

Table 1.1 Biochemical properties of phosphatidylinositol 4-kinase isoforms .....	12
----------------------------------------------------------------------------------	----

## ABBREVIATIONS

AP	adapter protein
ATP	adenosine triphosphate
AAT	Animal African Trypanosomiasis
BSF	bloodstream form
BSA	bovine serum albumin
CERT	ceramide transfer protein
DNA	deoxyribonucleic acid
DAG	diacylglycerol
DAPI	4',6-diamidino-2-phenylindole
DIC	differential interference contrast
dsRNA	double stranded RNA
EM	electron microscopy
ER	endoplasmic reticulum
EGF	epidermal growth factor
FBS	fetal bovine serum
FAZ	flagellar attachment zone
FP	flagellar pocket
GPI	glycosylphosphatidylinositol
GTP	guanosine triphosphate
HAT	Human African Trypanosomiasis
IP <sub>3</sub>	inositol triphosphate
kDa	kilodalton
LKU	lipid kinase unique
LDL	low density lipoprotein
mRNA	messenger RNA
μCi	microcurie
μl	microliter
μM	micrometer
ml	milliliter



mM	millimolar
MAP kinase	mitogen-activated protein kinase
MVB	multivesicular bodies
nm	nanometer
NGS	normal goat serum
ORF	open reading frame
OSBP	oxysterol binding protein
PBS	phosphate buffered saline
PI	phosphatidylinositol
PI(3,4,5)P <sub>3</sub>	phosphatidylinositol 3,4,5-trisphosphate
PI(3,4)P <sub>2</sub>	phosphatidylinositol 3,4-bisphosphate
PI(3,5)P <sub>2</sub>	phosphatidylinositol 3,5-bisphosphate
PI3-kinase	phosphatidylinositol 3-kinase
PI3P	phosphatidylinositol 3-monophosphate
PI(4,5)P <sub>2</sub>	phosphatidylinositol 4,5-bisphosphate
PI4-kinase	phosphatidylinositol 4-kinase
PI4KII- $\alpha$	phosphatidylinositol 4-kinase Type II-alpha
PI4KII- $\beta$	phosphatidylinositol 4-kinase Type II-beta
PI4KIII- $\alpha$	phosphatidylinositol 4-kinase Type III-alpha
PI4KIII- $\beta$	phosphatidylinositol 4-kinase Type III-beta
PI4P	phosphatidylinositol 4-monophosphate
PI5P	phosphatidylinositol 5-monophosphate
PIP	phosphatidylinositol phosphate
PIs	phosphoinositides
PLC	phospholipase C
PH	pleckstrin homology
PCR	polymerase chain reaction
PCF	procyclic form
PKC	protein kinase C
RNA	ribonucleic acid
RNAi	RNA interference
SEM	scanning electron microscopy

SDS-PAGE	sodium dodecyl sulfate polyacrylamide gel electrophoresis
SM	sphingomyelin
TIGR	The Institute of Genomic Research
TLC	thin layer chromatography
TGN	trans-Golgi network
TEM	transmission electron microscopy
Tb	Trypanosoma brucei
VSG	variable surface glycoprotein

# CHAPTER ONE

## Introduction

### ***A. Trypanosoma Brucei***

#### **1. Overview**

The parasitic protozoan, *Trypanosoma brucei*, is the causative agent of Human African Trypanosomiasis (HAT), also known as African Sleeping Sickness, and Animal African Trypanosomiasis (AAT) or Nagana. The parasite is transmitted to their mammalian hosts by the bite of an infected Tsetse fly (*Glossina* Spec.). HAT and AAT occur in 37 sub-Saharan countries, affecting nearly one third of the continent of Africa. Approximately 500,000 people are infected each year and it is estimated that 60 million people are at risk. Two subspecies infect humans, *Trypanosoma brucei rhodesiense*, found in west and central Africa, and *Trypanosoma brucei gambiense*, found in eastern and southern Africa. The sub-species *Trypanosoma brucei brucei* is pathogenic to animals and causes AAT in many species of wild and domestic animals. These animals can also be infected with the human infective sub-species *T. b. rhodesiense* and *T. b. gambiense* although they are not pathogenic in animals and therefore act as a reservoir for these parasites. Trypanosomiasis is a major obstacle to economic development in sub-Saharan Africa. Not only does it cause a loss of life in humans and livestock, but it also results in the abandonment of fertile grazing and farming land, which is infested with Tsetse flies. Drugs are available for the treatment of HAT, but these often have severe side-effects or are hard to administer. Safe and effective new treatments are needed not

only to save human lives, but also to aid in economic development and alleviation of poverty in affected areas ([www.who.int/en](http://www.who.int/en)).

## **2. African Trypanosomiasis**

The *T. brucei* parasites enter the bloodstream via the bite of the Tsetse fly. The parasites then begin to divide in the bloodstream and lymph system causing the first stage of the illness. This stage involves cyclical bouts of fever, headaches, joint pains and itching. Eventually the parasites cross the blood-brain barrier and infect the central nervous system, thereby initiating the second stage of the disease. This stage is characterized by the appearance of neurological symptoms including confusion, poor coordination, changes in personality and disturbance of the sleep cycle. As the disease progresses, neurological functions continue to deteriorate, resulting in coma and eventually death, if not treated.

There are two forms of HAT, depending on the sub-species of *T. brucei* involved. *T. b. rhodesiense* causes a more acute form of the disease, with onset of symptoms being within weeks to months of infection. Symptoms are severe and the infection progresses rapidly to the CNS stage. *T. b. gambiense* causes a more chronic infection and accounts for about 90% of HAT cases. Infected individuals can be asymptomatic for months and sometimes even years. Once symptoms do appear the disease is often in an advanced stage and permanent damage may have already occurred. Early detection and treatment of both forms of HAT are essential for survival. The first stage of the disease is treated with suramin in *T. b. rhodesiense* and pentamidine in *T. b. gambiense*. Once the parasite has crossed the blood-brain barrier it is much harder to treat. Merarsoprol treats the

second stage infection in both forms of HAT, but it is an arsenic based compound and has some severe side-effects that can even result in death. Eflornothine treats second stage infection, but only in the *T .b. gambiense* form of the infection. This drug is well tolerated, but the treatment regimen is strict and takes weeks ([www.who.int/en](http://www.who.int/en)).

### **3. *T. brucei* Biology**

The *T. brucei* parasite exists in two distinct life forms, the mammalian bloodstream form and the insect procyclic form. The parasites have a highly polarized exocytotic and endocytotic system, located between the nucleus and a specialized organelle called the flagellar pocket. This invagination of the plasma membrane near the posterior of the cell is the only site of exocytosis and endocytosis (Gull 2003). Both forms of the parasite express a stage-specific GPI-anchored surface protein (Cross 1975; Stebeck and Pearson 1994). The bloodstream form parasites are able to undergo antigenic variation by switching the expression of their variable surface glycoproteins, thereby evading the human immune response (Stebeck and Pearson 1994). Procyclic form parasites express two isoforms of the procyclic acidic repetitive protein procyclin, which is believed to protect the parasite from harsh environment of the fly midgut (Gruszynski, van Deursen et al. 2006). Mitochondrial function is differentially regulated in the different life stages. In the bloodstream form parasite, mitochondrial activity is repressed and ATP is generated from the host's blood glucose by glycolysis (Tielens and Van Hellemond 1998). Energy generation in the procyclic form switches from glycolysis to mitochondria cytochrome-dependent respiration and therefore this life stage has a more elaborate and active mitochondria than the bloodstream form (Matthews 2005).

## B. Phosphoinositides

Phosphoinositides (PIs), although minor constituents of eukaryotic cell membranes, play a crucial role in cellular regulation. PIs are phosphorylated derivatives of phosphatidylinositol, which can be differentially phosphorylated at the 3', 4', or 5' positions of the inositol ring, leading to seven possible phosphoinositides (Fig 1.1) (Fruman, Meyers et al. 1998). Their synthesis is partitioned at distinct subcellular locations within the cell and is mediated by specific phosphoinositide kinases and/ or phosphatases. These distinct pools function in localized recruitment of effector proteins to target membranes through interactions of the headgroup with lipid binding domains in their target proteins (De Matteis and Godi 2004).

PI3P, PI4P and PI(3,5)P<sub>2</sub> are predominately associated with intracellular membranes (Downes, Gray et al. 2005). PI3P is synthesized by the Type III PI3-kinase and is predominantly associated with the early endosomal system of mammalian cells and yeast (Gillooly, Morrow et al. 2000). In addition to its role in endosomal trafficking it also regulates Golgi to lysosome/vacuole sorting (Bravo, Karathanassis et al. 2001). PI3P interacts specifically with most FYVE domains and PX domains (Downes, Gray et al. 2005). PI4P can be synthesized by four different PI4-kinase isoforms in mammalian cells and three enzymes in yeast. Its main function is at the Golgi, where it is involved in the recruitment of proteins involved in vesicle budding and fission, and non-vesicular lipid transport (Balla and Balla 2006). PI(3,5)P<sub>2</sub> is synthesized from PI3P by a Type III PI3P 5-kinase (PIKFYVE) (Downes, Gray et al. 2005). PI(3,5)P<sub>2</sub> is implicated in multiple functions, including; retrograde transport from the vacuole to the endosome,

vacuole acidification, and ubiquitin-dependent protein sorting into multivesicular bodies (Phelan, Millson et al. 2006).  $\text{PI}(3,4)\text{P}_2$  and  $\text{PI}(3,4,5)\text{P}_3$  mediate PI3-kinase-dependent signaling pathways. Upon receptor activation,  $\text{PI}(3,4,5)\text{P}_3$  is synthesized from  $\text{PI}(4,5)\text{P}_2$  at the plasma membrane by Type I PI3-kinase. Synthesis of  $\text{PI}(3,4,5)\text{P}_3$  rapidly and transiently recruits effector proteins to the plasma membrane through interactions with their PH domains (Lemmon 2003).  $\text{PI}(3,4,5)\text{P}_3$  regulates multiple cellular processes, including cell growth and proliferation, cell movement and cell survival (Cantley 2002).  $\text{PI}(3,4)\text{P}_2$  is produced by the dephosphorylation of  $\text{PI}(3,4,5)\text{P}_3$  by SHIP and SHIP2 (Mitchell, Gurung et al. 2002).  $\text{PI}(3,4)\text{P}_2$  mediates many of the same PI3-kinase-mediated events as  $\text{PI}(3,4,5)\text{P}_3$ , but also has functions independent of  $\text{PI}(3,4,5)\text{P}_3$ , including regulation of sensitivity (Clement, Krause et al. 2001). The majority of  $\text{PI}(4,5)\text{P}_2$  is synthesized from  $\text{PI4P}$  by the Type I PIP 5-kinases, although there is evidence that  $\text{PI}(4,5)\text{P}_2$  can be synthesized from  $\text{PI5P}$  by the Type II PIP kinases (Oude Weernink, Schmidt et al. 2004).  $\text{PI}(4,5)\text{P}_2$  is the substrate for the phospholipase C enzymes, which results in the production of diacylglycerol (DAG) and 1,4,5-triphosphate ( $\text{IP}_3$ ). Production of these important second messengers results in the activation of protein kinase C (PKC) and intracellular calcium release.  $\text{PI}(4,5)\text{P}_2$  also has multiple cellular functions within the cell, including exocytosis and endocytosis, vesicular trafficking and actin cytoskeleton rearrangement (Toker 1998).

## **C. Phosphatidylinositol 4-Kinase**

### **1. Overview**

Phosphatidylinositol 4-kinases phosphorylates phosphatidylinositol at the 4' position, resulting in the production of phosphatidylinositol 4-monophosphate (PI4P) (Fig 1.2). Subsequent phosphorylation at the 3' and or 5' position, results in the synthesis of PI(3,4)P<sub>2</sub>, PI(4,5)P<sub>2</sub> and PI(3,4,5)P<sub>3</sub>. Recently it has been shown that PI4P is a lipid mediator in its own right, and not just a precursor molecule as was previously believed (Wang, Wang et al. 2003). The D4 phosphorylated PIs are essential lipid mediators for the regulation of multiple cellular functions, including; endocytosis, vesicular trafficking, actin cytoskeletal organization and Ca<sup>2+</sup> signaling (Toker 2002). Eukaryotes possess multiple isoforms of PI4-kinase, belonging to two different families, the Type II and Type III families. These two families can be distinguished by their sequences, biochemical properties and inhibitor profiles (Gehrmann and Heilmeyer 1998). Most eukaryotes possess at least one Type II enzyme, mammalian cells possess two (PI4KII- $\alpha$  and PI4KII- $\beta$ ) and most cells also have two Type III enzymes (PI4KIII- $\alpha$  and PI4KIII- $\beta$ ). Each of these enzymes localizes to distinct subcellular locations, where they regulate distinct cellular functions (Balla and Balla 2006).

## **2. Phosphatidylinositol 4-kinase Isoforms**

Vertebrates express two isoforms of the Type II enzymes, PI4KII- $\alpha$  and PI4KII- $\beta$ , while yeast express a single isoform, Lsb6b (Barylko, Gerber et al. 2001; Minogue, Anderson et al. 2001; Shelton, Barylko et al. 2003). The Type II enzymes are smaller, approximately 55 kDa and are tightly bound to the membrane, although they are not integral membrane proteins. These enzymes are palmitoylated on a conserved stretch of cysteine residues in the catalytic domain, which allows for association with the



membrane (Barylko, Wlodarski et al. 2002). The Type II enzymes show little sequence similarity to the Type III enzymes. The Type II enzymes are insensitive to the PI3-kinase inhibitor wortmannin, but are inhibited by adenosine (Table 1.1) (Balla and Balla 2006). These enzymes also have lower  $K_m$  values for their substrates ATP and PI, compared to the Type III enzymes (Table 1.1). The two Type III enzymes are structural relatives of the PI3-kinases and contain a lipid kinase unique domain (LKU) and the highly conserved C-terminal PI 3/4-kinase catalytic domain (Fig 1.3) (Balla and Balla 2006). PI4KIII- $\alpha$ , the larger of the two enzymes, also has a PH domain located between the LKU and the catalytic domain (Fig 1.3) (Wong and Cantley 1994).

### **3. Cellular Functions of Phosphatidylinositol 4-kinase Isoforms**

The Type II enzymes localize to the trans-Golgi network (TGN) and the endosome, where they are involved with the regulation of intracellular trafficking events (Balla, Tuymetova et al. 2002; Wang, Wang et al. 2003). In mammalian cells, synthesis of PI4P by PI4KII- $\alpha$  is required for the recruitment of clathrin adaptor AP-1 complexes to the Golgi (Wang, Wang et al. 2003). PI4KII- $\alpha$  is also required for recruitment of AP-3 to the endosomes (Salazar, Craige et al. 2005). The Type II enzymes are also implicated in transferrin receptor endocytosis and recycling, and EGF receptor degradation (Balla, Tuymetova et al. 2002; Minogue, Waugh et al. 2006).

The yeast ortholog of PI4KIII- $\alpha$ , Stp, is predominantly located at the plasma membrane and is important for maintaining cell wall integrity, actin cytoskeletal rearrangement, and for the PKC-mediated MAP kinase signaling cascade (Audhya, Foti et al. 2000). In mammalian cells the majority of the PI4KIII- $\alpha$  localizes to the ER,

although its role at the ER is not known at this time (Wong, Meyers et al. 1997). PI4KIII- $\alpha$  also functions at the plasma membrane, where it is responsible for the synthesis of the plasma membrane pool of PI4P (Balla, Tuymetova et al. 2005). It is postulated that the PI4KIII- $\alpha$  is the isoform involved in the synthesis of PI(4,5)P<sub>2</sub> for PLC-mediated DAG and IP<sub>3</sub> production (Nakanishi, Catt et al. 1995).

Pik1, the yeast ortholog of PI4KIII- $\beta$ , localizes to the nucleus and to the Golgi, where it is involved in the regulation of secretion (Hama, Schnieders et al. 1999; Walch-Solimena and Novick 1999; Audhya, Foti et al. 2000). The mammalian enzyme also localizes to the Golgi (Wong, Meyers et al. 1997; Godi, Pertile et al. 1999), and the nucleus (de Graaf, Klapisz et al. 2002), and regulates Golgi to plasma membrane trafficking (Bruns, Ellis et al. 2002; Godi, Di Campli et al. 2004). PI4KIII- $\beta$  is recruited to the Golgi by the small GTP-binding protein Arf1 (Godi, Pertile et al. 1999). PI4KIII- $\beta$  binds the GTP-bound form of Rab-11 and recruits it to the Golgi. Synthesis of PI4P by PI4KIII- $\beta$  at the Golgi is important for lipid transport in other eukaryotes (Toth, Balla et al. 2006). Synthesis of sphingomyelin (SM) from ceramide in the Golgi, requires CERT (ceramide transfer protein)-dependent transfer of ceramide from the ER (Levine and Munro 2002). CERT is localized to the Golgi membrane through its PH domain, which binds specifically to PI4P. Oxysterol-binding proteins (OSBPs) also bind specifically to PI4P through their PH domains. OSBP localizes to the Golgi apparatus in response to oxysterols, this interaction is PI4P and Arf1-dependent (Lagace, Byers et al. 1997; Levine and Munro 1998; Godi, Di Campli et al. 2004). Localization to the Golgi activates

CERT-dependent transport of ceramide to the Golgi, thereby integrating sterol homeostasis and SM synthesis (Perry and Ridgway 2006).

#### **D. Phosphoinositides in *T. brucei***

Currently little is known about the roles of phosphoinositides in *T. brucei*. The class III PI3-kinase was recently identified in *T. brucei* and depletion by RNAi implicated it in Golgi segregation and endocytotic trafficking. Like yeast, *T. brucei* do not have class I or II PI3-kinases, suggesting that *T. brucei* do not have PI3-kinase-dependent signaling pathways (Hall, Gabernet-Castello et al. 2006). Four putative PIP-kinases have been identified in the *T. brucei* genome. *T. brucei* have a Type I PI4P 5-kinase and a Type III PI3P 5-kinase (PIKFYVE). In addition to these two enzymes, the parasite has two Type II enzymes, both of which are most similar to the Type II PIP kinase- $\alpha$  isoforms. The presence of these enzymes indicates that *T. brucei* can theoretically synthesize all of the mono- and bis-phosphorylated phosphoinositides. Earlier studies in permeabilized procyclic cells revealed the presences of IP<sub>3</sub>, although there was no IP<sub>3</sub>-dependent release of intracellular Ca<sup>2+</sup>. It has been postulated that *T. brucei* does not use IP<sub>3</sub> as a second messenger or it has other functions (Moreno, Docampo et al. 1992).

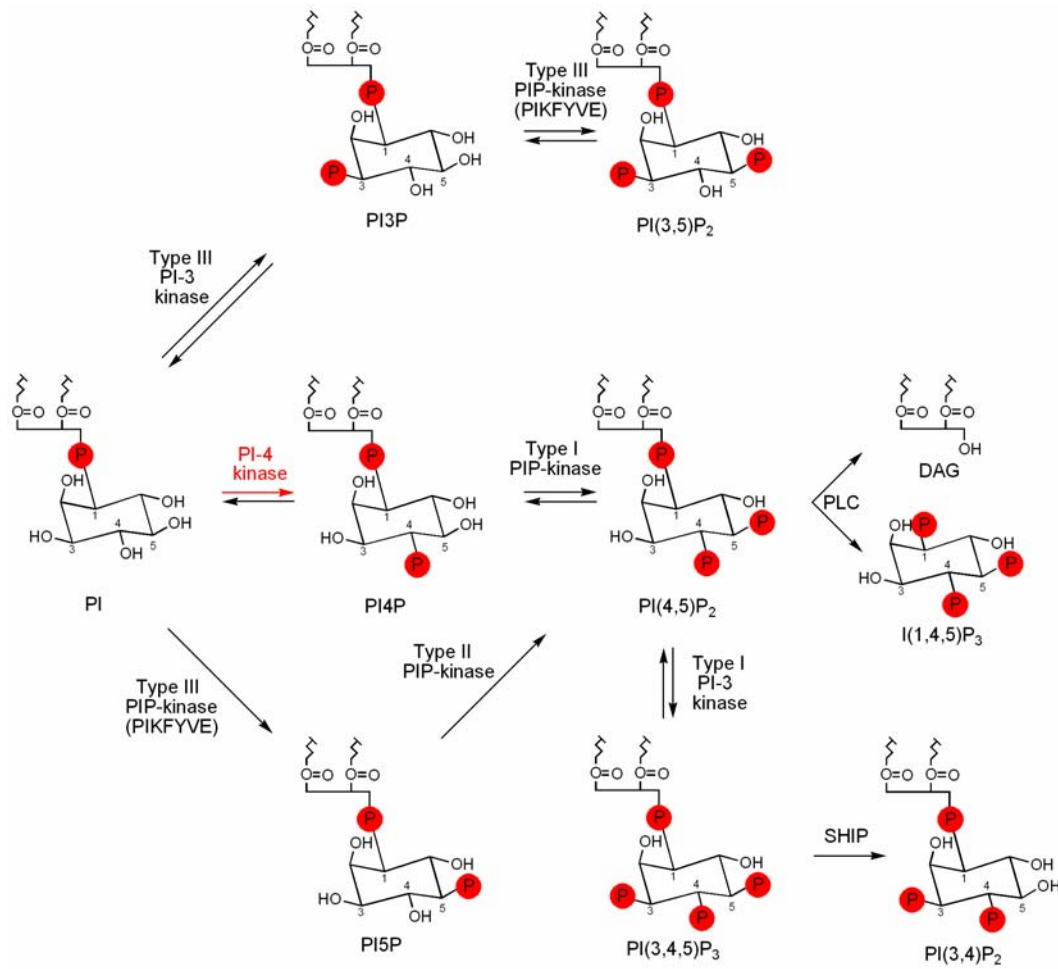


Figure 1.1. Phosphoinositide Cycle.

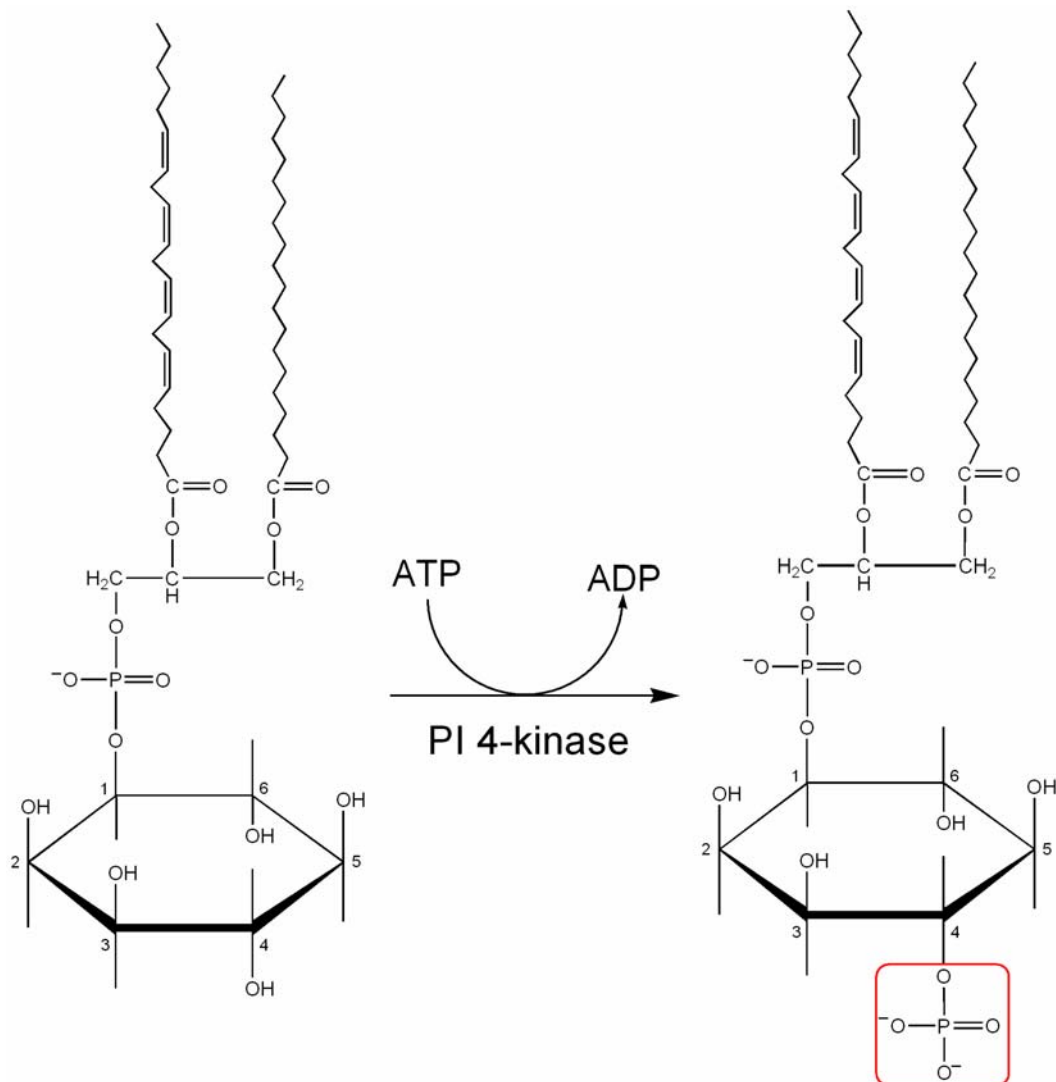
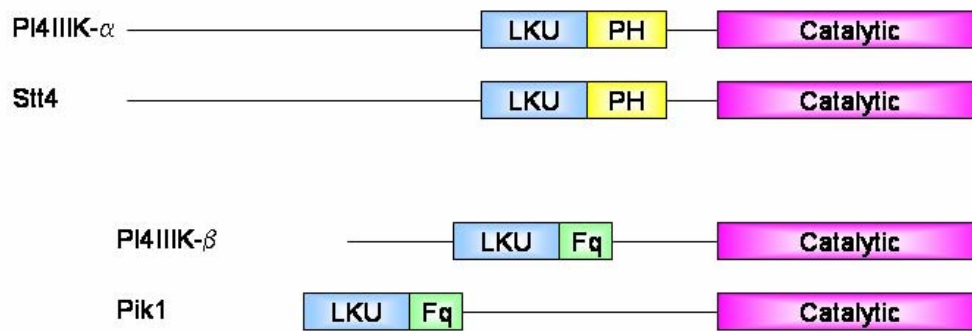


Figure 1.2. Phosphatidylinositol 4-kinase reaction.

	PI4KII- $\alpha$	PI4KII- $\beta$	PI4KIII- $\alpha$	PI4KIII- $\beta$
Molecular Weight	55-56 kDa	55-56 kDa	210-230 kDa	92-110 kDa
Wortmannin	Insensitive	Insensitive	IC <sub>50</sub> 50-300 nM	IC <sub>50</sub> 50-300 nM
LY-294002	Insensitive	Insensitive	IC <sub>50</sub> 50-100 $\mu$ M	IC <sub>50</sub> 100 $\mu$ M
K <sub>i</sub> Adenosine	10-70 $\mu$ M	10-70 $\mu$ M	>mM	>mM
K <sub>m</sub> ATP	10-50 $\mu$ M	10-50 $\mu$ M	~700 $\mu$ M	~400 $\mu$ M
K <sub>m</sub> PI	20-60 $\mu$ M	20-60 $\mu$ M	~100 $\mu$ M	~100 $\mu$ M

Table 1.1. Biochemical properties of phosphatidylinositol 4-kinase isoforms. (Balla and Balla 2006)

### Type III Enzymes



### Type II Enzymes

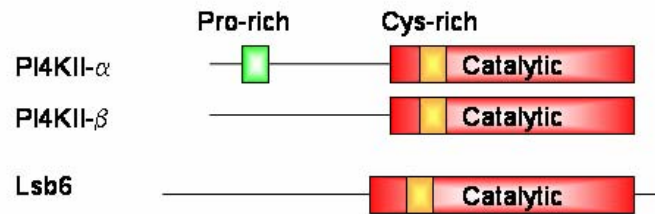


Figure 1.3. Domain structure of phosphatidylinositol 4-kinase isoforms. (Balla and Balla 2006)

## CHAPTER TWO

### Identification and Characterization of *T. brucei* PI4KIII- $\beta$

#### A. Introduction

Phosphatidylinositol 4-kinase phosphorylates phosphatidylinositol at the D4 position resulting in phosphatidylinositol 4-monophosphate. Subsequent phosphorylation events result in a group of molecules known as phosphoinositides. Recently it has been shown that PI4P is a lipid mediator in its own right, and not just a precursor molecule as was previously believed (Wang, Wang et al. 2003). The D4 phosphorylated phosphoinositides are essential lipid mediators, which regulate multiple cellular functions, including; endocytosis, vesicular trafficking, actin cytoskeletal organization and  $\text{Ca}^{2+}$  signaling (Toker 1998). Eukaryotes possess multiple isoforms of PI4-kinases, belonging to two different families, the Type II and Type III families. These two families can be distinguished based on their sequences, biochemical properties and inhibitor profiles (Gehrmann and Heilmeyer 1998). Most eukaryotes possess at least one Type II enzyme, mammals possess two (PI4KII- $\alpha$  and PI4KII- $\beta$ ) and two Type III enzymes (PI4KIII- $\alpha$  and PI4KIII- $\beta$ ). Each of these enzymes localizes to distinct subcellular locations, where they regulate distinct cellular functions. (Balla and Balla 2006).

Currently very little is known about the phosphoinositide cycle or the enzymes involved in *T. brucei*. Recently the putative Class III PI3-kinase was identified in *T. brucei* and was shown to be required for normal growth in bloodstream cells (Hall, Gabernet-Castello et al. 2006). In this study, we identified both Type III PI4-kinases in



The Institute of Genomic Research (TIGR) *T. brucei* database. Northern analysis revealed that TbPI4KIII- $\alpha$  and TbPI4KIII- $\beta$  are expressed at similar levels in both life stages. TbPI4KIII- $\beta$  was further characterized after cloning and protein expression. Recombinant protein was able to phosphorylate phosphatidylinositol, thereby confirming that TbPI4KIII- $\beta$  is an authentic PI4-kinase.

## **B. Materials and Methods**

### **1. Cell Culture**

Procyclic culture form (PCF) *T. brucei brucei* Lister 427 cells were grown in SDM-79 media (Brun and Schonenberger 1979). PCF 29-13 cells (a generous gift of George Cross, Rockefeller University), were grown at 25°C in SDM-79 media, supplemented with 10% FBS, in the presence of 25  $\mu$ g/ml G418 (Sigma) and 25  $\mu$ g/ml hygromycin (A.G. Scientific). Cells were grown to log phase ( $5-10 \times 10^6$  cells/ml) and diluted 1:50 every 3-4 days into fresh media.

Bloodstream form (BSF) 90-13 cells (a generous gift of George Cross, Rockefeller), were grown at 37°C in HMI-9 media (Hirumi and Hirumi 1989), supplemented with 10% FBS in the presence of 2.5  $\mu$ g/ml G418 and 5  $\mu$ g/ml hygromycin. Cells were grown to log phase ( $5-10 \times 10^5$  cells/ml) and diluted 1:500 about every 2-3 days into fresh media.

### **2. Lysate Preparation**

Approximately  $2 \times 10^7$  log phase 427 PCF cells were harvested by centrifugation and washed one time with ice-cold phosphate buffered saline (PBS). The cell pellet was

resuspended in 500  $\mu$ l Buffer A (20 mM Tris-HCl, pH 7.5, 25 mM Sucrose, 100 mM NaCl, 1.0 mM EDTA, 1 mM NaVO<sub>3</sub>, 1mM DTT, 0.2 mM PMSF and PICI and PICII ). Lysates were subjected to three freeze/thaw cycles and were placed on ice for 30 minutes. Lysates were centrifuged at 70k rpm (Beckman T-100) for 15 minutes at 4°C. The supernatant (cytoplasmic fraction) was removed and the pellet was resuspended in 500  $\mu$ l of Buffer B (1% Triton X-100, 1% Glycerol, 20mM Tris-HCl, pH 7.5, 100 mM NaCl, 1 mM NaVO<sub>3</sub>, 1.0 mM DTT, 0.2 mM PMSF and PICI and PICII) and incubated on ice for 10 minutes. Lysates were centrifuged as above and the supernatant (membrane fraction) was removed.

### **3. In Vitro Kinase Assays**

Phosphatidylinositol/Triton X-100 micelles were prepared by sonicating phosphatidylinositol (PI) (Avanti) in Buffer C (50 mM Tris-HCl pH 7.5, 1.0 mM EGTA, 0.4% Triton X-100 and 0.5 mg/ml BSA). Reactions contained 10  $\mu$ l of lysate, 38  $\mu$ l PI/TritonX-100 micelles and were initiated with the addition of 2  $\mu$ l of ATP mix (50mM Tris-HCl pH7.5, 375 mM MgCl, 5 mM ATP and [  $\gamma$ -<sup>32</sup>P]ATP (10 mCi/mmol). The reaction contained 1mM PI, 200  $\mu$ M ATP and 15 mM MgCl and were carried out at room temperature for 30 min. For wortmannin inhibition, lysates were preincubated with 100  $\mu$ M wortmannin (Sigma) for twenty minutes at room temperature. After preincubation, the wortmannin concentration was adjusted so that the final concentration in the 50  $\mu$ l reaction was 100  $\mu$ M. For adenosine inhibition, reactions were carries out in the presence of 100  $\mu$ M adenosine (Sigma). Reactions were stopped by addition of 3.75 volumes of chloroform/methanol/HCl (100:200:1), followed by extraction with 1.25 volumes of

chloroform and of 0.1 N HCl. The lipids were separated by thin layer chromatography (TLC) using an n-propyl alcohol/H<sub>2</sub>O/NH<sub>4</sub>OH (65:20:15) solvent system and radioactive spots were detected by autoradiography, scraped, and quantified by scintillation counting.

#### **4. RNA Isolation and Northern Blot Analysis**

Total RNA was extracted from log-phase cultures using RNAqueous Kit (Ambion). 2 $\mu$ g of total RNA was separated on a 1% agarose/formaldehyde gel and transferred to BrightStar-Plus nylon membranes (Ambion). Hybridization was performed overnight at 42°C in ULTRAhyb hybridization buffer (Ambion). <sup>32</sup>P labeled probes for TbPI4KIII- $\alpha$ , TbPI4KIII- $\beta$  and  $\alpha$ -Tubulin were synthesized using StripEZ-DNA Random-Primed Stripable DNA Probe kit (Ambion). Blots were stripped and reprobed according manufacturer protocols. The dsDNA probes were designed to hybridize with the following regions of the transcripts; TbPI4KIII- $\alpha$ , 5712-6609; TbPI4KIII- $\beta$ , 1-675; and  $\alpha$ -Tubulin, 1-650. 4  $\mu$ g of RNA size markers (Ambion) were separated on the same gel and transferred to the membrane. In order to visualize the markers, the marker lane was cut off and stained with 0.03 % methylene blue solution. The stained markers were then used to determine the size of the mRNAs.

#### **5. Cloning and Expression**

TbPI4KIII- $\beta$  was identified by blasting The Institute for Genomic Research (TIGR) *T. brucei* database with the human PI4KIII- $\beta$  protein sequence (NP\_002642). An open reading frame was found on BAC clone RPCI93-5E12 from chromosome 4. Primer

sequences were designed to generate a PCR fragment coding for the complete coding region from 427 *T. brucei* genomic DNA, 5'-ATGTCGAATGCTTTGTTTTGTCTTCACAGG-3' and 5'-GAGTATAACCATTCTGGAGAG 3', which was then sub-cloned into the Zero Blunt TOPO PCR Cloning vector (Invitrogen) and sequenced.

The full length gene was amplified by PCR from 427 genomic DNA and sub-cloned into the mammalian expression vector pCMV-tag2b (Stratagene) using the primers 5'-GTTTCCTTTTCCGGATCCATGTCGAATGCTTTGTTTTG-3' AND 5'-CATTCACCACATCCCCTCGAGCTAGAGTATAACCATT-3', which contain restriction sites, BamHI and XhoI respectively. The fragment was sub-cloned in frame and downstream of the N-terminal Flag tag. COS-7 cells were grown in Dulbecco's Modified Eagle's Medium, supplemented with 10% FBS on 10 cm plates. Purified plasmid pCMV-tag2b or pCMV-TbPI4KIII- $\beta$ , containing the full-length TbPI4KIII- $\beta$  was transfected into COS-7 cells using Lipofectamine 2000 (Invitrogen) according to manufacturers protocols. Cells were incubated at 37°C in 5% CO<sup>2</sup> for 18 hrs.

## 6. Immunoprecipitation

COS-7 cells were washed with PBS and lysed on ice in Buffer A (20mM Tris-HCl, pH 7.5, 25 mM Sucrose, 100 mM NaCl, 1.0mM EDTA, 1 mM NaVO<sub>3</sub>, 1 mM DTT, 0.2 mM PMSF and PICI and PICII). After centrifugation (70k for 15 minutes at 4°C), Triton X-100 was added to the supernatant for a final concentration of 0.1%. 300  $\mu$ l of cleared lysate was incubated overnight with 75  $\mu$ l  $\alpha$ -Flag M2 resin (Sigma). Beads

were then washed 3 times with buffer A + 0.1% TritonX-100. Beads were then resuspended in 75  $\mu$ l Buffer A +0.1% TritonX-100, resulting in a 50% bead slurry.

## 7. Immune Complex Kinase Assays

Phosphatidylinositol/Triton X-100 micelles were prepared by sonicating PI (Avanti) in Buffer C (50 mM Tris-HCl, pH 7.5, 1.0 mM EGTA, 0.4% Triton X-100 and 0.5 mg/ml BSA). Reactions contained 10  $\mu$ l bead slurry, 38  $\mu$ l PI/TritonX-100 micelles and were initiated with the addition of 2  $\mu$ l of ATP mix (50mM Tris-HCl pH7.5, 375 mM MgCl, 5 mM ATP and [ $\gamma$ -<sup>32</sup>P]ATP (10 mCi/mmol). The reactions contained 200  $\mu$ M PI, 400  $\mu$ M ATP and 15 mM MgCl and were carried out at room temperature for 30 min. Reactions were stopped by addition of 3.75 volumes of chloroform/methanol/HCl (100:200:1), followed by extraction with 1.25 volumes of chloroform and of 0.1 N HCl. The lipids were separated by thin layer chromatography (TLC) using an n-propyl alcohol/H<sub>2</sub>O/NH<sub>4</sub>OH (65:20:15) solvent system and radioactive spots were detected by autoradiography, scraped, and quantified by scintillation counting.

## C. Results

### 1. Inhibitor Profile of PCF Lysates

*T. brucei* cell lysates were tested for phosphatidylinositol kinase activity. Activity was measured as the ability of lysates to transfer phosphate from [ $\gamma$ -<sup>32</sup>P]ATP to phosphatidylinositol in Triton X-100 micelles. Both the cytoplasmic and Triton X-100 solubilized membrane fractions phosphorylated phosphatidylinositol (Fig 2.1). The Type II and III isoforms can be distinguished by their inhibitor profiles. Procyclic cytoplasmic

and membrane lysates were inhibited by 100  $\mu$ M wortmannin and were not sensitive to 100  $\mu$ M adenosine. When lysates were treated with both inhibitors, inhibition was comparable to wortmannin alone. Sensitivity to wortmannin, but not adenosine is characteristic of Type III enzymes, and indicates that procyclic *T. brucei* lack the Type II enzymes.

## 2. Transcript levels

The two different life stages of *T. brucei* often differentially express mRNA. The two forms live in very different host environments and have therefore adapted to these differences. mRNA transcript levels for both TbPI4KIII- $\alpha$  and TbPI4KIII- $\beta$  were determined by northern blot analysis in bloodstream form 90-13 and procyclic form 29-13 (Fig 2.2). Transcripts for both TbPI4KIII- $\alpha$  and TbPI4KIII- $\beta$  were detected in both forms. The transcript for the larger of the enzymes, TbPI4KIII- $\alpha$ , was approximately 8.5 kb and the TbPI4KIII- $\beta$  transcript was approximately 2.5 kb (Fig. 2.2). Both transcripts are expressed at similar levels in both life forms.

## 3. Sequence Analysis

The gene for *T. brucei* PI4KIII- $\beta$  was identified through a BLAST search of the TIGR *T. brucei* database. The search originally identified an ORF of 1761 nucleotides in a BAC clone from chromosome 4. The deduced amino acid sequence encoded for a 581 amino acid protein with a predicted molecular mass of 66 kDa. CLUSTALW analysis revealed that the *T. brucei* enzyme shares 20.4% identity and 18.4% similarity with the

human enzyme. The predicted protein's domain structure was characteristic of the type III PI4-kinases, with a highly conserved C-terminal phosphatidylinositol 4-kinase catalytic domain and a less conserved lipid kinase unique domain (LKU) at the N-terminal (Fig 2.4-A). The catalytic domain shares 41% identity and 26.6% similarity with the human enzyme, whereas the LKU shares only 7.63% identity and 22.88% similarity. The catalytic domain sequence contained all but one of the required conserved residues, as predicted by Gehrman and Heilmeyer. In *T. brucei*, the conserved aspartic acid-11 (D11) is replaced by an asparagine residue (R11) (Fig 2.4-C). It is predicted that this residue helps to position the required catalytic lysine (K7), although this has not been experimentally determined in lipid kinases (Gehrmann and Heilmeyer 1998).

#### **4. Protein Expression and Characterization**

In order to confirm the identity of our gene we over expressed the protein in COS-7 cells, using the pCMV-tag2b (N-terminal Flag tagged) mammalian expression vector. The over expressed protein was immunoprecipitated out of COS-7 cell lysates using  $\alpha$ -Flag M2 resin (Sigma). The Flag-tagged product was only detected in the lysates from cells transfected with the pCMV-TbPI4KIII- $\beta$  vector and not cells transfected with empty vector (Fig 2.5). The flag-tagged product migrated on SDS-PAGE gel between the 75 kDa and 50 kDa marker, which correlates with the predicted molecular mass of 66 kDa. Phosphatidylinositol kinase assays were performed using the immunoprecipitated recombinant protein and showed that the expressed protein was able to phosphorylate phosphatidylinositol (Fig 2.6). The PI-kinase activity is wortmannin-sensitive, inhibited

by 100  $\mu$ M wortmannin. No phosphatidylinositol kinase activity was detected in the empty vector control immunoprecipitations.

#### **D. Discussion**

Two phosphatidylinositol 4-kinases were identified in *T. brucei*; TbPI4KIII- $\alpha$  and TbPI4KIII- $\beta$ . Northern blot analysis revealed that both enzymes are expressed in both life stages at similar levels. Unlike yeast and mammalian cells, it appears that *T. brucei* does not have a Type II enzyme. Activity of *T. brucei* lysates is wortmannin-sensitive and adenosine insensitive and the *T. brucei* database does not contain the sequence. Further database searches reveal that other members of the trypanosomatid family, including; *T. cruzi* and *L. major*, also lack a Type II sequence, indicating that functions regulated by the Type II enzymes in other organisms are regulated by the Type III enzymes in the trypanosomatids.

Primary sequence analysis suggested that we had cloned the *T. brucei* PI4KIII- $\beta$  and preliminary characterization of the activity of the overexpressed protein confirmed its identity. Although the overall conservation is low, 20.4% identity and 18.4% similarity to the human enzyme, the protein sequence has the characteristic domain structure seen in the Type III enzymes and contains the conserved lipid kinase catalytic domain and the more divergent lipid kinase unique domain (LKU). The conserved aspartic acid residue (D11), which is conserved in all lipid kinases, is an asparagine (N) in the *T. brucei* sequence. It is predicted that this residue is involved in positioning the catalytic lysine (K7 in Fig 2.4-C) in lipid kinases. The proper positioning of the required catalytic lysine is essential for activity (Gehrmann and Heilmeyer 1998). The TbPI4KIII- $\beta$  enzyme is



active, so it is likely that this is not is residue responsible in *T. brucei*. It was also noted that the *T. brucei* enzyme is substantially smaller than other PI4KIII- $\beta$  enzymes, with a smaller N-terminal region. Whether this effects enzymatic properties has yet to be determined.

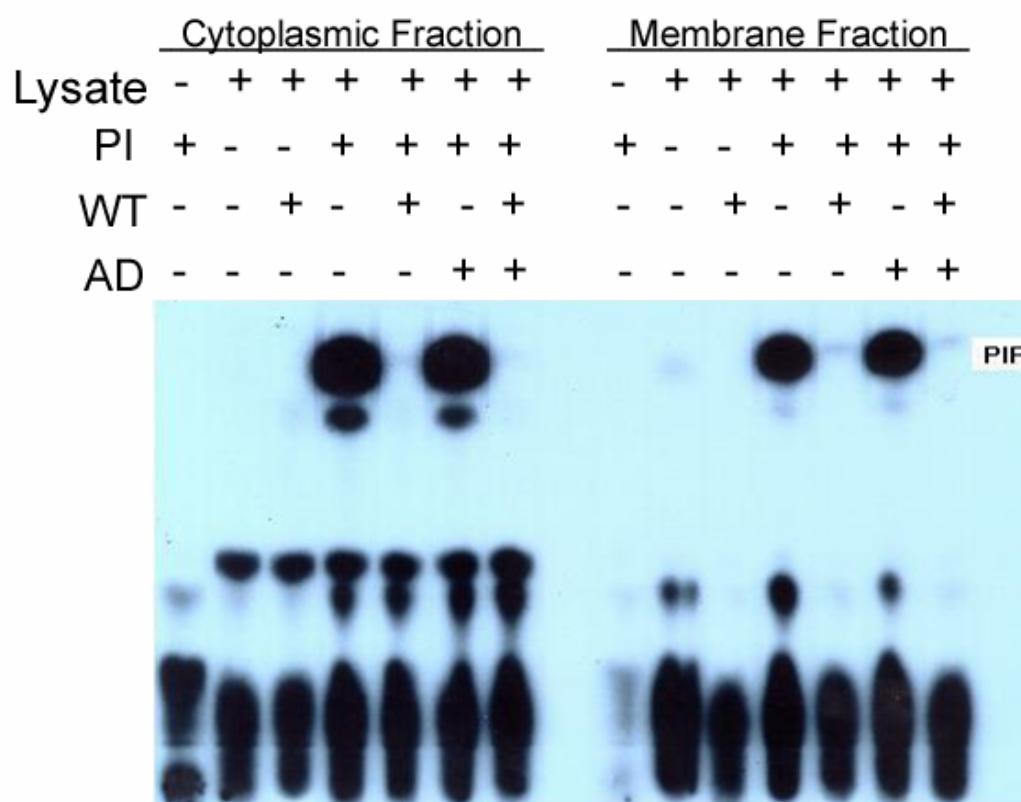


Figure 2.1. Endogenous phosphatidylinositol kinase activity. Reactions contained 10  $\mu$ l of lysate or buffer, 38  $\mu$ l PI/TritonX-100 micelles and were initiated with the addition of 2  $\mu$ l of ATP mix. The reaction contained 1mM PI, 200  $\mu$ M ATP and 15 mM MgCl and were carried out at room temperature for 30 min. Wortmannin (WT) 100  $\mu$ M and adenosine (AD) 100  $\mu$ M.

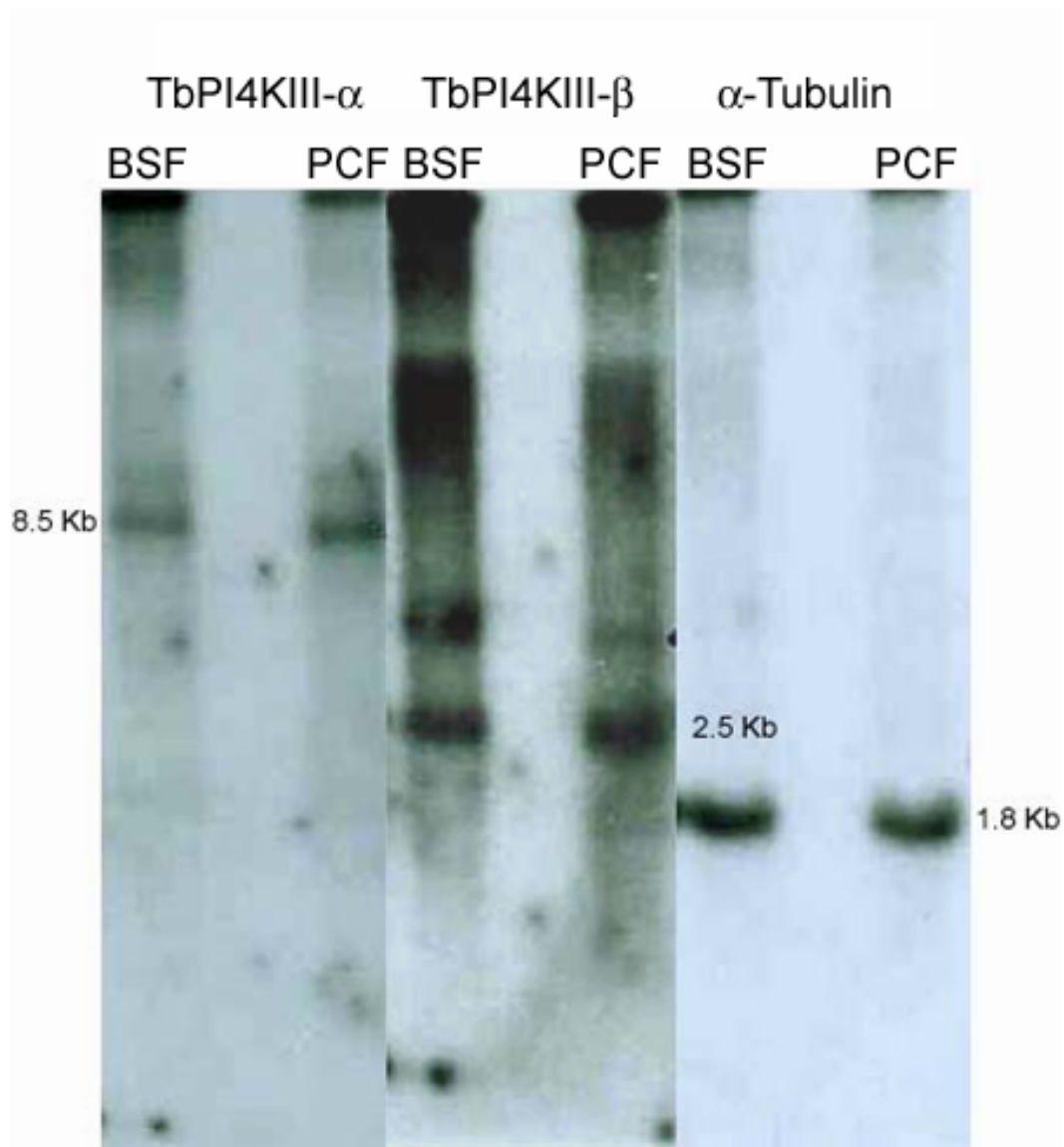


Figure 2.2. Northern blot analysis. 2 $\mu$ g of total RNA, bloodstream form (BSF) and procyclic form (PCF), was separated on a 1% agarose/formaldehyde gel and transferred to BrightStar-Plus nylon membranes. The blot was then probed for TbPI4KIII- $\alpha$ , TbPI4KIII- $\beta$  and  $\alpha$ -Tubulin. The transcript sizes are as follows: TbPI4KIII- $\alpha$ , 8.5 Kb; TbPI4KIII- $\beta$ , 8.5 Kb; and  $\alpha$ -Tubulin, 1.8 Kb.

atgtcgaatgctttgtttgtcttcacaggcttctggaggtactgctgtacctaccgagg  
 M S N A L F C L H R L L E V L L Y L P R  
 ggttctcaggatgagcaaatggctcttggtcaaaatctgcatgagttcccccttgcaacc  
 G S Q D E Q M A L V Q N L H E F P L A T  
 attgaaaggggtcttccttcaaatatctcatgcttgatcacgcacaaggggtccggaggta  
 I E R V F L Q I S H A C I T H K G P E V  
 agtaaccgcctgcgacgttttatgcattggctggcggggcgatcttttaccttggcggtg  
 S N R L R R F M H W L A G R S F T L A L  
 cggctctcatggacagtggactcggtagcgacgtgttttcggccgttgggcttggaggg  
 R L S W T V D S V R D V F S A V G L G G  
 cgcgtgaaggaagtgcacgacaagatcgagagttttgccatcaaccgcaaggggtgtagca  
 R V K E V H D K I E S F A I N R K G V A  
 gatcgaaccaacaactgacggggtagaggaagagattaggcgcaaggaactgacgactt  
 D R T N N T D G V E E E I R R K E L R L  
 aagcttttcaacgatgagagagcatttcctcaatcttatcaccaacttgagtaaacttta  
 K L F N D E R A F L N L I T N L S K H L  
 atttcgttcaccaagagagatcggcgacaacatgagctaaagaaggagctggatgaaatc  
 I S F T K R D R R Q H E L K K E L D E I  
 aacaaatcactgaggtcgcagtcactcatatgccctttgggttgtaatgacgatccggta  
 N K S L R S Q S L I C P L G C N D D P V  
 aagtggattgtaaactcggttggtgaagatagtgctgattcttttctcgtgagagagcg  
 K W I V N I V V E D S V V F F S R E R A  
 ccgtttctccttcgatgcgaagtcattgttgattccactgcaactgtcaatgaccaact  
 P F L L R C E V I V D S T A T V N D P T  
 acatctaagttacgacttcccaatggaaagtttaaaatttcggcggaatcagatgaattg  
 T S K L R L P N G K F K I S A E S D E L  
 atggaggagcagtcgctggaccgaaggggggaagatgtaggaggggaggttaactgcatc  
 M E E Q S L D R R G E D V G G E V T A I  
 aagtccgcttccctgacatgaagttggttcggaaggtctttggagagcttccggaggaa  
 K A S P D M K L F R K V F G E L P E E  
 cgagctgctcgtctgcgcgagaagtcattctttgggagggcatcctaattggggtacagcc  
 R A A R L R E K S F F G R H P N W G T A  
 acatttgtgggtcaaaggtggagataatttgcggcaagaggagttggcggttacaacttgtt  
 T F V V K G G D N L R Q E E L A L Q L V  
 gacctcttcaacaatatatggaagaatgccggacttacatgctctcttgtcccctatagg  
 D L F N N I W K N A G L T C S L V P Y R  
 gcacttgcgctcgggtgtggattctggaattattgagtgtgtagaggggtgcctgttccatt  
 A L A V G V D S G I I E C V E G A C S I  
 gatggaatcaagaagtcatgtcagatggcgtaccttccccagttcttcaatgaggccttt  
 D G I K K S C Q M A Y L P Q F F N E A F  
 ggtggcaaggggtcccaaagatatagggagggtcagcgaaatttcgtggagacaatggct  
 G G K G S Q R Y R E A Q R N F V E T M A  
 ggttacagtatctttacctatatacttcagggtgaaagatagacacaacgggaacattttg  
 G Y S I F T Y I L Q V K D R H N G N I L  
 ataagggcagacggccgtttggtgcacatagactttggttttatgctcgtcacatctccc  
 I R A D G R L V H I D F G F M L V T S P  
 ggtggtgtcaacttcgaatcagcccccttcaaactgtcacaagagctccttgaagtaatg  
 G G V N F E S A P F F K L S Q E L L E V M  
 ggaaggtgttgaagttcaccatttaattactttaagctattgttcttcttggggatgaga  
 G G V G S S P F N Y F K L L F F L G M R

```

gccatacgcgagaaaagctgatgatatcgtagcacttgtctcgctaatacgccttacaac
  A I R E K A D D I V A L V S L M T P Y N
actttgccttgtttcggggcctctcctgaagttgccatccagcaactgcggtcccgcctt
  T L P C F G A S P E V A I Q Q L R S R F
cgtttggatctagaggacgagggagatttgcactttatattaaggaactcattgtcgg
  R L D L E D E G D F A L Y I K E L I V G
agtgtggacaactggaggacgagggcggtacgatcagttccaaactctccagaatggata
  S V D N W R T R R Y D Q F Q T L Q N G I
ctctag
L -

```

Figure 2.3. The nucleotide and translated amino acid sequence of the full-length PI4KIII- $\beta$ . The amino acid sequence is shown using the single letter abbreviation. The sequence for TbPI4KIII- $\beta$  is available from GenBank™ (XM\_839171).

A.



B.

```

TbPI4KIIIIBeta  evLLYiprgsqdeQiaLvqnLheFPlAtIErvflQIshacItHKgpEVSnrLrrFmhwa
HsPI4KIIIIBeta  IsyLYnsk-epGVQaYigNRLfcFrnedVdfYlpQllnMyI-HmdedVgdAikpYIvhrC
AtPI4KIIIIBeta  VsyLYkhp-haGVrdYLCNRmytlPlSgIESYlfQIcyMmv-HKp---SpSLDKFVidiC
ScPI4KIIIIBeta  VeLLckhseniGIhyYLCqKLAtFPhSelqfYlpQlvqVlv-tmetE-SmAEdlLlrlr

TbPI4KIIIIBeta  grSftlALrlsWtvdsrvrdvfSavglggFvkEvhdkIesfAInrkG
HsPI4KIIIIBeta  rQSInFsLqcallLgAyssDm-----hISTqrh-
AtPI4KIIIIBeta  gkSlkiALkvhWfllAeLeDaddnegisRiQEkC----qIAatlmG
ScPI4KIIIIBeta  aEnphFALLtfWqLqAlltDlStdpasygFQvarrvLnnLqTNlf-

```

C.

```

ScPI4KIIIIBeta  LcSVIAktGDDLRLQeafAyQMIqamaNIWvKekvdVwvKrmKILITSantGLvEtItNAm
TbPI4KIIIIBeta  tatfvVKgGDnLRQeELALQLVdlFnNIWknAgLtcsLvPYRaLavgvdsGsiECvegAc
HsPI4KIIIIBeta  lLSVIVKcGDDLRLQeELafQvklqlqsIWeQervPLWiKPYKILViSAdSGmIEpvnNAV
AtPI4KIIIIBeta  LrSIIVKsGDDcRQeHLavQLIshEydIfqEAgLPLWLRPyEVLVTSSytaLIETIpdtA

ScPI4KIIIIBeta  SvHSIKKaltkkniedaelddkkgIaSLnDhFlraFGnpNgfkyRrAQdNFasSLAaYSv
TbPI4KIIIIBeta  SIIdgIKKscq-----mayLpqFFneaFGgkgSgryReAQORNFVETMAGYSi
HsPI4KIIIIBeta  SIHqvKKqsg-----lSLDYFlqehGsytTeaFlsAQORNFVQSCAGYcL
AtPI4KIIIIBeta  SIHSIKsrypn-----ItSLrDFFvakY-keNSpsFKLAQORNFVESMAGYSL

ScPI4KIIIIBeta  ICYLLQVKDRHNGNImIDnEGHVSHIDFGFMLSNSPGSvVGFEaAPFKLTyEyiEl1----
TbPI4KIIIIBeta  ftYiLQVKDRHNGNILIrAdGr1VHIDFGFMLvtSPGGVnFESAPFKLsqELIEVM----
HsPI4KIIIIBeta  VCYLLQVKDRHNGNILLdaEGHIIHIDFGFiLSsSPrnlgFEtsaFKLTtEfvdVM----
AtPI4KIIIIBeta  VCYLLQVKDRHNGNILLDeEGHIIHIDFGFMLSNSPGGVnFESAPFKLTreLIEVMdsda

ScPI4KIIIIBeta  GGVeGEaFkkFveLtkssFkAlRKYAdqIVsmcEIMQkdNmqPCFdAGeQtsvQ-LRQRF
TbPI4KIIIIBeta  GGVgsspFNYFKlLfflGmrAiRekAdDlVaLVsLMtpyNtlPCFgAsPEvaIQgLRsRF
HsPI4KIIIIBeta  GGldGDmFNYYKmLmlqGliAaRKHmDkvVqiVEIMQqgsqLPCFhgss--TlrNLKERF
AtPI4KIIIIBeta  dGVpsEfFdYFKvLciqGFeltcRKHAerIilLVEmlQ-dsgfPCFkgGPr-TIQNLRKRF

ScPI4KIIIIBeta  qLDLSEk-EvddfVenfliGkSLgSIyTRiYDqFQlitqGIys
TbPI4KIIIIBeta  rLDLedEgdfalyikELIvG-SvdNwrTRrYDqFQtLqNGIL-
HsPI4KIIIIBeta  HmsmTEE-QlqlLveQMvDg-SMrSiTtklYDgFQyLtnGIM-
AtPI4KIIIIBeta  HLsLTEE-QcvsLVlsLIss-SLdAwrTRqYDyyQrvlNGIL-

```

Figure 2.4. Domain structure of TbPI4KIII- $\beta$  and MUSCLE alignments. (A) TbPI4KIII- $\beta$  has the typical PI4KIII- $\beta$  domain structure; an N-terminal lipid kinase unique domain (LKU) and a C-terminal catalytic domain. The sequence alignments were prepared using

the MUSCLE alignment program (<http://www.bioinformatics.nl/tools/muscle.html>); (A) LKU alignment and (B) catalytic domain alignment. The protein sequences were from the following species; *T. brucei* (XP\_844264), *H. sapien* (NP\_002642), *S. cerevisiae* (NP\_014132), and *A. thaliana* (NP\_201212).

## $\alpha$ -Flag Western Blot

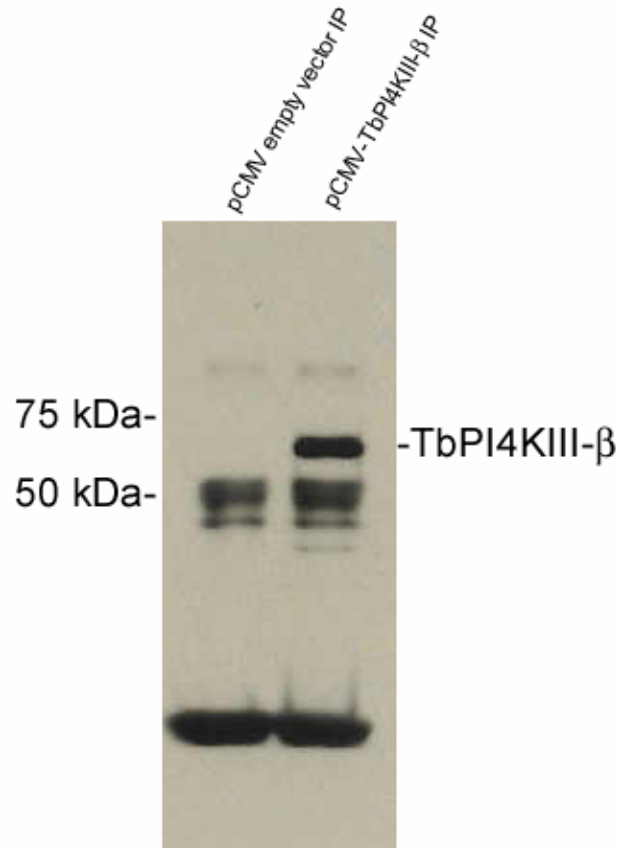


Figure 2.5. Western blot of immunoprecipitated Flag-tagged recombinant TbPI4KIII- $\beta$ . Recombinant TbPI4KIII- $\beta$  was immunoprecipitated out of COS-7 cell lysates using  $\alpha$ -Flag M2 resin and analyzed by western blot. The  $\alpha$ -Flag antibody detected a band which migrated on SDS-PAGE gel between the 75 kDa and 50 kDa marker in the pCMV-TbPI4KIII- $\beta$  lane. No recombinant protein was detected in the empty vector control lane.



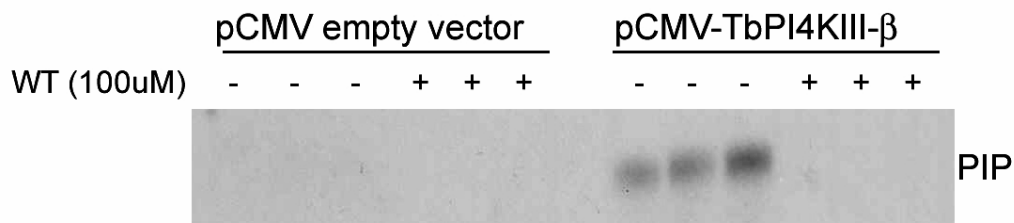


Figure 2.6. Immune complex kinase assay of Flag-tagged recombinant TbPI4KIII- $\beta$ . Immunoprecipitated proteins were tested for phosphatidylinositol (PI) kinase activity. The recombinant TbPI4KIII- $\beta$  protein was able to phosphorylate PI, no activity was seen in the empty vector control samples. The activity was inhibited by 100  $\mu$ M wortmannin (WT). The reactions contained 200  $\mu$ M PI, 400  $\mu$ M ATP and 15 mM MgCl and were carried out at room temperature for 30 min.

## CHAPTER THREE

### Generation of TbPI4KIII- $\beta$ RNAi Cell Line

#### A. Introduction

RNA interference is a well established tool for genetic manipulation of *Trypanosoma brucei*. RNAi in was originally achieved by electroporation of *in vitro* synthesized dsRNA (Ngo, Tschudi et al. 1998). This was soon followed by the introduction of inducible, stably maintained constructs that express dsRNA as a stem-loop structure or through the of opposing T7 promoters to produce it (Shi, Djikeng et al. 2000; Wang, Morris et al. 2000; Bastin, Galvani et al. 2001). These constructs are transfected into a cell line expressing the tetracycline repressor and T7 polymerase, and are integrated into the non-transcribed ribosomal DNA spacer region of the genome (Wang, Morris et al. 2000). The expression of dsRNA is under the control of either the tetracycline-inducible PARP promoter in the stem-loop construct, or opposing tetracycline-inducible T7 promoters (Wirtz and Clayton 1995; Shi, Djikeng et al. 2000; Wang, Morris et al. 2000; Bastin, Galvani et al. 2001). Induction of dsRNA expression leads to gene-specific degradation of targeted mRNA. The inducible and stable expression of dsRNA and subsequent decrease in transcript levels in *T. brucei* allows for investigation of gene function in a reliable and reproducible fashion (Shi, Djikeng et al. 2000; Wang, Morris et al. 2000; Bastin, Galvani et al. 2001). In order to investigate the functional role of TbPI4KIII- $\beta$  in procyclic *T. brucei*, a TbPI4KIII- $\beta$  RNAi cell line was

generated using a tetracycline-inducible PARP promoter stem-loop vector in procyclic *T. brucei*. Tetracycline induction led to selective reduction of TbPI4KIII- $\beta$  mRNA transcripts levels within 24 hours, followed by a subsequent decrease in phosphatidylinositol 4-monophosphate levels. Depletion of TbPI4KIII- $\beta$  results in a growth defect, rounded phenotype and eventually leads to cell death, indicating that TbPI4KIII- $\beta$  is an essential enzyme in Procyclic *T. brucei*.

## **B. Materials and Methods**

### **1. Cell Culture and Transfection**

Procyclic culture form (PCF) 29-13 cells (a generous gift of George Cross, Rockefeller University), which stably express T7 polymerase and a tetracycline repressor, were used for creating RNAi cell lines (Wirtz, Leal et al. 1999). 29-13 parental line cultures were grown in SDM-79 supplemented with 10% FBS, in the presence of 25  $\mu$ g/ml G418 and 25  $\mu$ g/ml hygromycin. 29-13 cells were transfected with EcoRV linearized RNAi plasmid, using a BioRad Gene Pulser II at 1.5 kV, 25  $\mu$ F in 0.4 cm electrocuvettes (BioRad). After electroporation, transfectants were selected for by culturing cells in the presence of 2.5  $\mu$ g/ml phleomycin in addition to G418 and hygromycin. Synthesis of RNA was induced by the addition of tetracycline at 1  $\mu$ g/ml (Wang, Morris et al. 2000).

### **2. Plasmid Construction**

Primers were designed to amplify the coding region between positions 421-1002 of the DNA sequence. 5'-GGAAGTGC GACTTAAGCTTTTCAACGATGAGAG-3'

and 5'-GCTAGCTCCTCTTGCCGCAAAT-3' contain restriction sites HindIII and NheI respectively. This fragment was then sub-cloned into the HindIII and NheI sites of pJM326 (a generous gift of Paul Englund, Johns Hopkins University). The complementary strand was amplified using primers 5'-GGAAGTGCCTTACGCGTTTCAACGATGAGAG-3' and 5'-TCTAGATCCTCTTGCCGCAAAT-3', which contain restriction sites for MluI and XbaI, respectively. This fragment was sub-cloned into the MluI and XbaI sites in pLew100 (a generous gift of Paul Englund, Johns Hopkins University). The pJM326 construct containing our insert was digested with HindIII and XbaI, releasing a larger fragment containing the target gene fused to a stuffer fragment. This fragment was then sub-cloned into the HindIII and XbaI sites in the pLew100 construct containing the complement of the target gene (Fig. 3.1)

### 3. RNA Isolation and Northern Blot Analysis

Total RNA was extracted from log-phase cultures using RNAqueous Kit (Ambion). Total RNA samples were collected from tetracycline-induced cultures every 24 hrs., over six days. Total RNA was also collected from an uninduced culture. 2µg of total RNA was separated on a 1% agarose/formaldehyde gel and transferred to BrightStar-Plus nylon membranes (Ambion). Hybridization was performed overnight at 48°C in ULTRAhyb hybridization buffer (Ambion). <sup>32</sup>P labeled probes for TbPI4KIII-β and α-Tubulin were synthesized using StripEZ-PCR probe synthesis kit (Ambion). Blots were stripped and re-probed according manufacturer protocols. The dsDNA probes were designed to hybridize with the following regions of the transcripts; TbPI4KIII-β, 1-

675; and  $\alpha$ -Tubulin, 1-650. 4  $\mu$ g of RNA size markers (Ambion) were separated on the same gel and transferred to the membrane. In order to visualize the markers, the marker lane was cut off and stained with 0.03 % methylene blue solution. The stained markers were then used to determine the size of the mRNAs.

#### **4. Growth Curves**

For growth curves, cell counts were performed using a hemocytometer. Three independent experiments were counted and the averages were reported.

#### **5. Inositol Labeling**

Mid-log phase trypanosomes from uninduced cultures, and cultures induced for three and five days were centrifuged at 400xg and washed once with PBS. Trypanosomes were resuspended in 5 ml fresh SDM-79 supplemented with 10% FBS at  $2 \times 10^7$  cells/ml, and 50  $\mu$ l of 10  $\mu$ Ci/ $\mu$ l  $^3$ H-myo-inositol (Amersham) was added to the mixture, and incubated for 24 hrs at 25°C. Cells were centrifuged at 400xg, washed with PBS and the supernatant removed. Lipids were extracted with 375  $\mu$ l of methanol:HCL (1:1) and 190  $\mu$ l of chloroform. The lipids were separated by thin layer chromatography (TLC) using an n-propyl alcohol/H<sub>2</sub>O/NH<sub>4</sub>OH (65:20:15) solvent system and radioactive spots were detected by autoradiography, scraped, and quantified by scintillation counting. The ratio of PI/PIP was calculated for 5 independent experiments at each time point and averaged.

### **C. Results and Discussion**

#### **1. TbPI4KIII- $\beta$ RNAi Cell line**

In order to investigate possible functional roles of TbPI4KIII- $\beta$  in procyclic *T. brucei*, we generated a stable tetracycline-inducible RNAi procyclic cell line. We used an RNAi vector which produces dsRNA as a stem-loop structure in procyclic form *T. brucei* (Fig 3.1) (Wang, Morris et al. 2000). This construct contains a region of our target gene (nucleotides 421-1002) and its complement separated by a stuffer region. The linearized vector was transfected into 29-13 procyclic *T. brucei* by electroporation and transfectants were selected for using phleomycin. Upon induction with the addition of tetracycline, an RNA is transcribed which can then fold into a stem-loop structure. This dsRNA containing the target gene sequence and then targets the mRNA for degradation (Wang, Morris et al. 2000).

The effects of RNAi on TbPI4KIII- $\beta$  were initially examined by northern blot analysis. Total RNA was collected from log phase cultures in the absence and presence of tetracycline. After 24 hours of tetracycline induction, transcript levels are virtually undetectable, compared to the uninduced cells (Fig 3.2). The transcript levels remain undetectable throughout 6 days of induction.

## **2. Depletion of TbPI4KIII- $\beta$ Causes a Defect in Growth**

Cell growth was monitored through cell counts over a two week period. Induced cells began to show a defect in growth and an abnormal morphology after four days of induction. The growth defect continues, although around day eight, growth begins to pick up. These cultures are not clonal and therefore are a mixed population. Microscopic analysis of the cultures revealed that after day eight the abnormal looking cells are dying and a population of what look like normal cells begins to grow up. This is a common

problem with procyclic RNAi cell cultures, which consist of an RNAi-positive population and a wild-type population that is RNAi-negative. It is likely that upon induction, the RNAi-positive population eventually dies off, while the RNAi-negative population continues to grow. Eventually, after continued induction with tetracycline, one is left with a homogeneous population of RNAi-negative cells. Although our growth curve does not continue to show a decrease in cell number after day eight, we know that cells displaying the abnormal phenotype die and therefore we believe that depletion of TbPI4KIII- $\beta$  in procyclic cells is lethal.

### **3. Depletion of TbPI4KIII- $\beta$ Results in a Decrease in PI4P**

To demonstrate the depletion of TbPI4KIII- $\beta$  results in a decrease in phosphatidylinositol-monophosphate (PIP) levels, PIP levels were monitored by inositol labeling. Uninduced and induced cells were incubated with  $^3\text{H}$ -inositol for 24 hrs. The lipids were then extracted, separated by TLC and quantitated by scintillation counting. PIP levels were then normalized against PI in order to account in different cells numbers in the samples. PIP levels were decreased by 20% after four days of induction and 70% after six days, indicating that induction of RNAi of TbPI4KIII- $\beta$  does result in a decrease in PIP Levels. The decrease in PIP levels correlates with the timing of the appearance of the growth defect and the abnormal phenotype, indicating that the synthesis of PI4P by TbPI4KIII- $\beta$  is required for proper growth and morphology. *T. brucei* has two PI4-kinases, PI4KIII- $\alpha$  and PI4KIII- $\beta$ , both of which contribute to total PIP levels. The

decrease of PI4P by 70% at 6 days, indicates that TbPI4KIII- $\beta$  is responsible for the majority of PIK activity in procyclic form *T. brucei*.



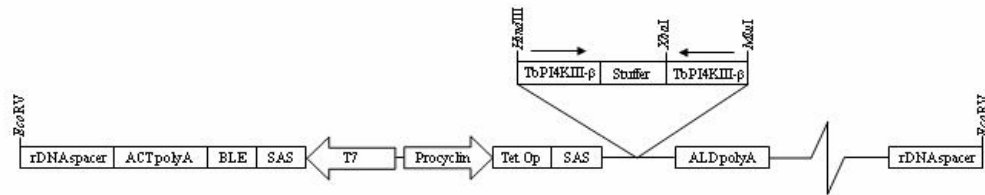


Figure 3.1. Stem-loop vector construct. This construct contains a region of our target gene (nucleotides 421-1002) and its complement separated by a stuffer region. Transcription of the dsRNA is mediated by a tetracycline-inducible procyclin promoter.

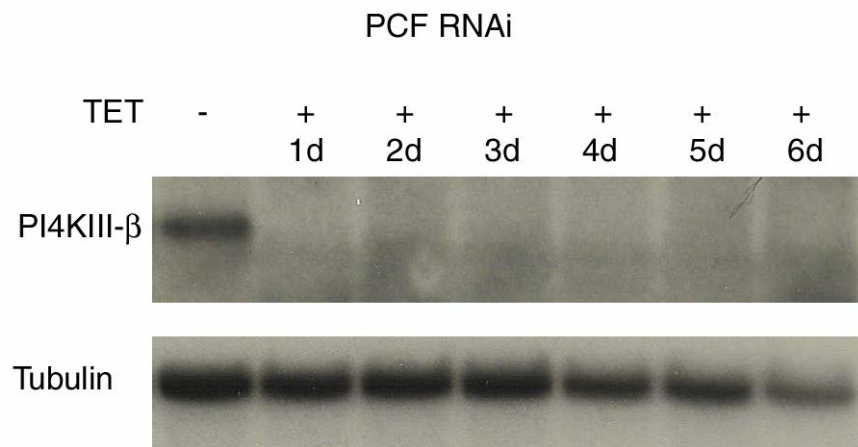


Figure 3.2. Northern blot analysis of TbPI4KIII- $\beta$  RNAi cells. Transcript levels from samples collected over six days of tetracycline induction were determined. 2 $\mu$ g of total RNA was separated on a 1% agarose/formaldehyde gel and transferred to BrightStar-Plus nylon membranes. The blot was then probed for TbPI4KIII- $\beta$  and  $\alpha$ -Tubulin. After 24 hrs of induction, transcripts for TbPI4KIII- $\beta$  were undetectable and remained that way through day six.

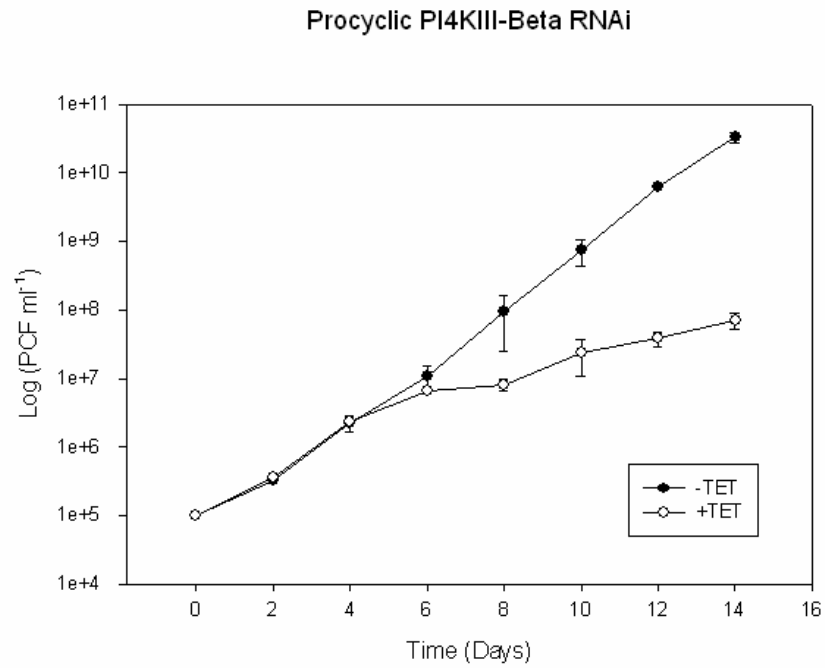


Figure 3.3. Effect of TbPI4KIII- $\beta$  depletion on growth. Cell growth was monitored for uninduced (-TET) and induced (+TET) cells over two weeks. Induced cells (-TET) showed a defect in growth beginning at day four.

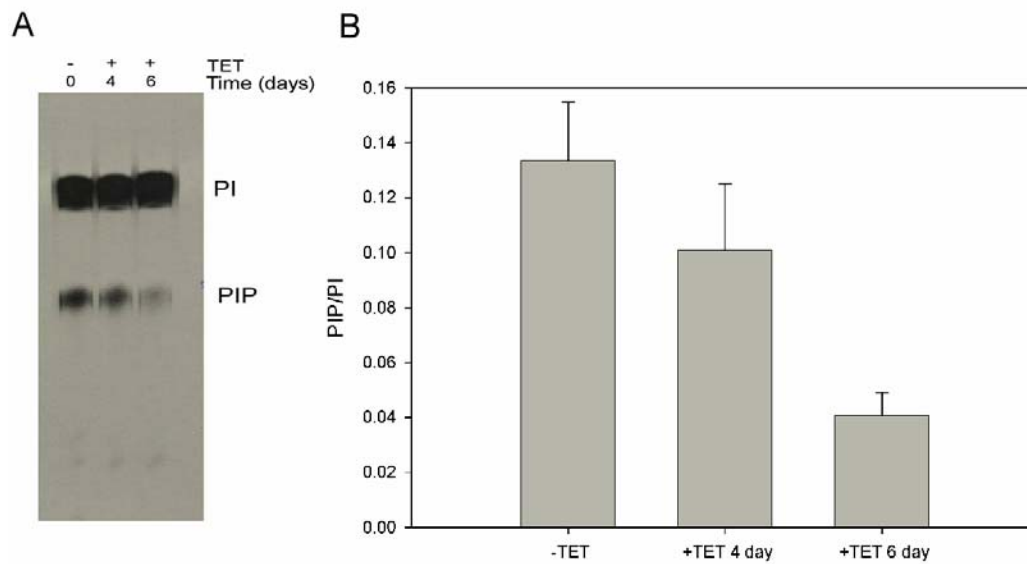


Figure 3.4. Effect of TbPI4KIII- $\beta$  depletion on phosphatidylinositol monophosphate levels. Phosphatidylinositol monophosphate (PIP) levels were monitored by inositol labeling. Uninduced cells and cells induced for three and five days were incubated with  $^3\text{H}$ -inositol for 24 hrs. The lipids were then extracted, separated by TLC, and quantitated by scintillation counting. Autoradiograph of TLC separated lipids (A). PIP levels were normalized against PI levels to account for differences in cell number. Each bar represents the average of five independent experiments, error bars represent standard deviation (B). After four days of induction PIP levels were reduced by 20% and by six day. Levels were reduced by 70%.

## CHAPTER FOUR

### **TbPI4KIII-b is Required for Normal Morphology in Procyclic**

#### **A. Introduction**

The long and slender cell shape of the trypanosome is maintained by a complex subpellicular corset of cytoplasmic microtubules underlying the plasma membrane. The subpellicular microtubules are cross-linked to each other and to the plasma membrane, and remain intact throughout the entire cell cycle (Sherwin and Gull 1989). These microtubules have the same polarity and are orientated such that the dynamic plus ends are located at the posterior and the minus ends at the anterior end of the parasite (Sherwin and Gull 1989; Robinson, Sherwin et al. 1995). All of the developmental stages of *T. brucei* have a similar cell organization characterized by the presence of several single copy organelles (Vickerman and Preston 1970). The motile flagellum emerges from the flagellar pocket in the posterior region of the cell and runs along the entire length of the cell body. The flagellar pocket is the only region of the cell where the plasma membrane is not linked to the subpellicular microtubules, thus allowing for membrane dynamics and therefore is the only site of endocytosis/exocytosis in *T. brucei* (Overath and Engstler 2004). The single basal body is located at the base of the flagellum and is physically linked to the compact mitochondrial DNA known as the kinetoplast (Kohl, Sherwin et al. 1999; Ogbadoyi, Robinson et al. 2003). The single elongated mitochondria, extends from the posterior to the anterior of the cell. Located between the flagellar pocket and the

nucleus is a single Golgi stack, the lysosome and the endosomal compartments. *T. brucei* also have an extensive endoplasmic reticulum, which extends throughout the interior of the cell (Matthews 2005).

The distinct cellular architecture of *T. brucei* and the precise positioning of the organelles within the cell are fundamental to cellular function and survival. Alterations in this architecture are often lethal in this organism. Examination of cells depleted of TbPI4KIII- $\beta$  revealed an abnormal morphology, characterized by an accumulation of internal vesicles and a twisted cell shape. Immunofluorescence and electron microscopy were employed to investigate this morphological defect in detail.

## **B. Materials and methods**

### **1. Cell Culture**

The TbPI4KIII- $\beta$  RNAi cell cultures were grown at 25°C in SDM-79 supplemented with 10% FBS in the presence of 25  $\mu$ g/ml G418, 25  $\mu$ g/ml hygromycin and 2.5  $\mu$ g/ml phleomycin. Synthesis of RNA was induced by the addition of tetracycline at 1  $\mu$ g/ml (Wang, Morris et al. 2000).

### **2. Immunofluorescence Microscopy and Phenotype Quantitation**

The methods for preparation of slides and imaging are described in detail in Chapter 5. Cells were examined using a Zeiss Axiovert 200M inverted microscope equipped with a Zeiss 100x numerical aperture oil immersion objective, and a CCD camera. Digital images were captured and analyzed using Slidebook 4.0 software (Intelligent Imaging Innovations) and images were prepared with Adobe Photoshop (5.5).

In order to determine the frequency of the phenotype, a population of one hundred cells at each time was counted, and normal, fat and round phenotypes were scored.

### **3. TEM**

Cells for transmission electron microscopy were fixed in suspension by adding 5% glutaraldehyde and 6.4% paraformaldehyde in PBS to trypanosomes in an equal volume of growth medium. Cells were then rinsed, pelleted, and embedded in 2% agarose. Small pieces of cell pellet were post-fixed with 1% osmium tetroxide, dehydrated in a graded ethanol series, and embedded in EMbed-812 resin. Thin-sections were cut on a LEICA EM UC6 ultramicrotome, post-stained with uranyl acetate and lead citrate, and viewed in a JEOL JEM-1200EX electron microscope operating at 80 kV.

### **4. SEM**

Cells for scanning electron microscopy were fixed in suspension by adding 5% glutaraldehyde and 6.4% paraformaldehyde in phosphate PBS to trypanosomes in an equal volume of growth medium. Cells were then adhered to poly-L-lysine coated coverslips, post-fixed in 1% osmium tetroxide, dehydrated in a graded ethanol series, and transferred through several changes of hexamethyldisilazane (HMDS). Specimens were allowed to air-dry overnight, sputter-coated with gold and viewed in a JEOL JSM-840A SEM.

## **C. Results**

### **1. DIC Images of the Phenotype**

Light microscopic analysis of induced cultures showed the appearance of an abnormal phenotype around day 4 (Fig 4.1). The phenotype is comprised of fat and round cells. The frequency of the phenotype increases over time, resulting in a heterogeneous population of cells consisting of normal, fat and round morphologies (Fig-4.2). After six days of induction, approximately 60% of the population has an abnormal fat or round shape. By day seven, approximately 85 % of the cells have an abnormal phenotype. The morphologically abnormal cells also had a motility defect. Cells were not able to move through media, instead staying in one place and spinning in circles.

## 2. Ultrastructural Analysis

*T. brucei* maintain a well defined cell architecture, with most of the major organelles located between the flagellar pocket and the nucleus (Fig 4.3-A-B). Ultrastructural analysis of TbPI4KIII- $\beta$  depleted cells revealed that the cytoplasm of these cells was filled with numerous vesicles of varying size (Fig-4.3-C-E). The vesicles vary in number and in size from approximately 50 nm to 750 nm. Most of the vesicles are lucent, although some do have electron-dense materials (Fig 4.3-C). Some resemble acidocalcisomes, while others appear similar to multivesicular bodies (MVB). There is also the accumulation of abnormal membrane structures within the cytoplasm (Fig 4.3-F). The morphology of the major organelles, the kinetoplast, flagellum, flagellar pocket and nucleus appear to be normal (Fig 4.3-C-D), but their normally polarized organization within the cell is lost. The shapes of the cells vary; most are expanded and have lost their normally slender appearance (Fig-4.3-C-E). There is also the accumulation of abnormal



membrane structures within the cytoplasm and many of the cells had an abnormal accumulation of vesicles within the flagellar pocket (Fig 4.3-F).

### **3. Scanning Electron Microscopy**

Scanning electron microscopy was employed in order to examine the surface structure of the induced cells. Uninduced trypanosomes normally appear as long and slender cells. Their cell shape is defined by a highly polarized microtubule cytoskeleton (Matthews 2005). The microtubules are organized length-wise, with the minus end at the anterior and the plus ends at the posterior of the cell (Robinson, Sherwin et al. 1995). The flagellum can be seen originating from the flagellar pocket at the posterior end and running the length of the organism (Fig 4.4-A). The SEM images revealed an aberrant morphology with a unique characteristic. Depletion of TbPI4KIII- $\beta$  resulted in a twisted phenotype, which appears to begin at the posterior end of the parasite and over time results in a twisted round cell (Fig 4.4-B-D). This twisted phenotype is seen in thin and round cells (Fig 4.4-B-D), and in dividing and non-dividing cells (Fig 6.6). Uninduced cells, which are progressing through the cell cycle can be detected by the presence of the daughter flagellum/flagellar pocket and the cleavage furrow (Fig 6.6-A). Induced cells progressing through the cell cycle also have a second flagellum/flagellar pocket, but the daughter flagellum is sometimes detached (Fig 6.6-B-C). The presence of a cleavage furrow has not been detected in the TbPI4KIII- $\beta$ , indicating that cytokinesis may be defective in these cells.

### **4. Examination of Abnormal Surface Structure**

Electron microscopy revealed abnormal membrane structure in a subpopulation of cells. TEM revealed that the surface of these cells was no longer smooth but had protrusions (Fig 4.5-A-B). The underlying subpellicular microtubules can be seen in these images. SEM revealed a similar surface abnormality, with what look like protrusions and indentations in the membrane. These cells appear to show the progression of the morphological defect, which ultimately results in the cells collapsing in on themselves. Similar cells were not observed in the uninduced cells.

#### **D. Discussion**

Depletion of TbPI4KIII- $\beta$  in procyclic *T. brucei* results in severe morphological abnormalities. The fat/round phenotype begins around day four. This correlates well with the decrease in PIP levels seen in the inositol labeling experiments. The frequency of the abnormal phenotype increases over time, resulting in a population of mostly round cells by day seven. This indicates that the fat phenotype is most likely a precursor to the round cells. Ultrastructural analysis revealed that the cytoplasm of abnormal shaped cells was filled with a heterogeneous population of vesicles. The size and shape of the vesicles vary greatly. Some of the vesicles were lucent, while others appeared to contain electron dense material. Many of the vesicles resembled acidocalcisomes, which are normally found in *T. brucei* in small numbers. Acidocalcisomes are electron-dense acidic organelles, which contain high concentrations of calcium and polyphosphate and are implicated in several functions, including storage of cations and phosphorus, calcium homeostasis, and regulation of intracellular pH homeostasis and osmolarity (Docampo, de Souza et al. 2005). The increase in the number of these organelles might be the result

of osmotic stress or a change in intracellular pH. Although most of the major organelles were present, their positioning was abnormal. The normally polarized organelle structure was lost in these cells. It should be noted that we were not able to visualize the Golgi in the abnormal cells, indicating a possible defect. Many of the vesicles seen in the abnormal cells may have orientated from the Golgi and may be transport intermediates. TbPI4KIII- $\beta$  is well known to function at the Golgi in other organisms and it is very likely that it functions at the Golgi in *T. brucei*. Although the structure of the flagellar pocket looked relatively normal, there was often the accumulation of vesicles inside the pocket. Structures which resembled MVBs were also detected nearby indicating possible defects in endocytosis and the endosomal system.

SEM revealed that the fat and round cells were actually twisted. This abnormal morphology seemed to progress over time, finally resulting in a twisted round cell. This abnormality may be caused by a defect in the microtubule cytoskeleton, which maintains the shape of the cell. The twist is seen in both non-dividing and dividing cells, indicating that it is not cell cycle dependent. Some of the cells were not fat or round and appeared relatively normal except for the twist. This indicates that the twist seems to begin before the cells become fat or round. It begins at the posterior of the cell, which is where the flagellum originates from the flagellar pocket. It is possible that a defect in the structure, attachment or movement of the flagellum could cause the abnormal surface structure. The flagellum is physically attached to the surface of the cell in a helical pattern. Abnormal flagellar attachment and subsequent movement may induce this helical pattern in the cell surface.

Depletion of TbPI4KIII- $\beta$  in procyclic *T. brucei* causes multiple morphological defects. Phosphoinositides regulate many processes and the depletion of D4 phosphoinositides would affect multiple processes. The different defects we see in these cells are probably due to the disruption of multiple pathways. It is obvious that TbPI4KIII- $\beta$  is required for normal morphology, but at this time we do not know the exact mechanisms of the defects.

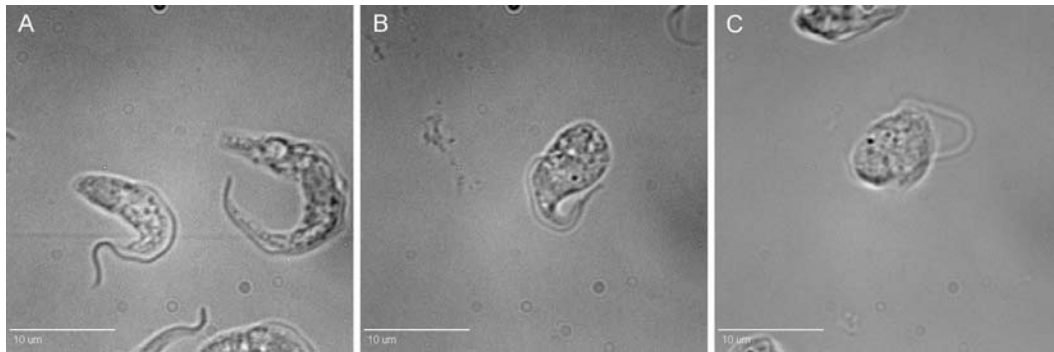


Figure 4.1. TbPI4KIII- $\beta$  is required for normal morphology in procyclic *T. brucei*. Brightfield DIC microscopy reveals an abnormal phenotype in cells depleted of TbPI4KIII- $\beta$ ; Normal phenotype, uninduced cells (A), fat phenotype and round phenotype (C). Both (B) and (C) are from cultures induced for six days. Scale bar 10  $\mu$ m.

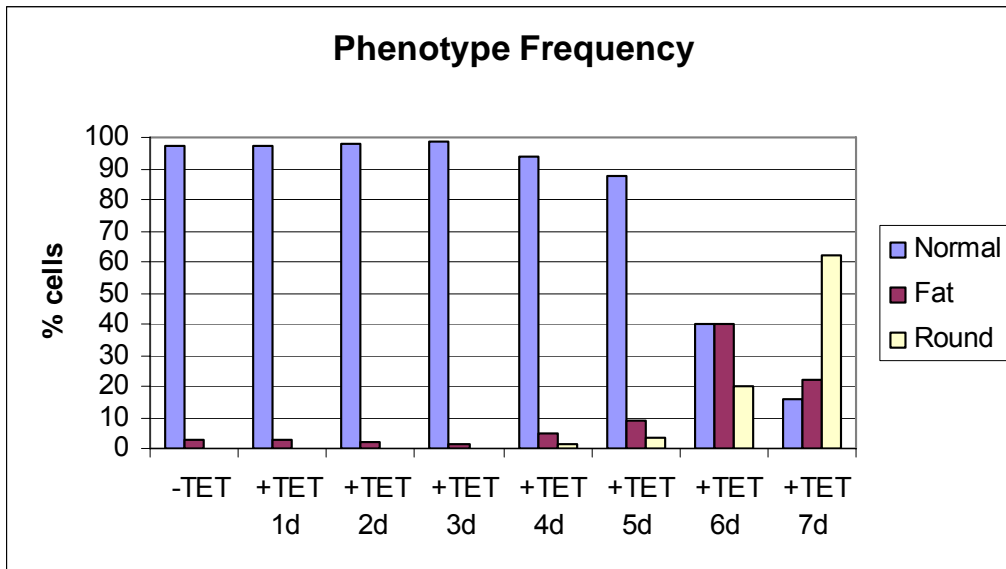


Figure 4.2. Frequency of phenotypes in induced cultures. The frequency of three phenotypes (normal, fat and round) was determined over one week of induction. At day four the percentage of the fat and round begin to increase and by day seven approximately 85% of the cells have an abnormal phenotype.

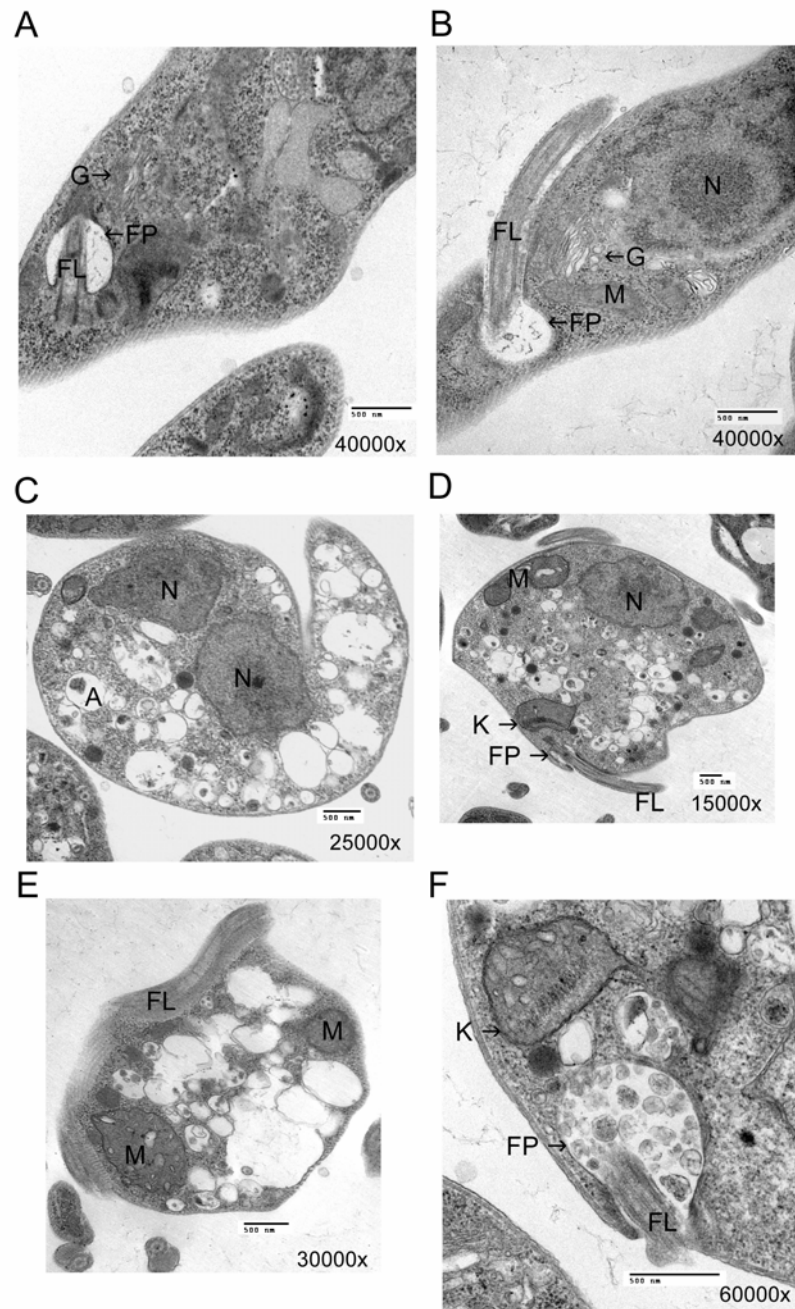


Figure 4.3. Ultrastructural analysis of *TbPI4KIII-β* depleted cells. Transmission electron microscopy was used to examine the ultrastructure of uninduced cells (A-B) and cells induced for six days (C-F). Cells depleted of *TbPI4KIII-β* display are abnormally shaped and their cytoplasm is filled with vesicles (C-E). There is also an accumulation of

vesicles in the flagellar pocket (F). Abbreviations: FP, flagellar pocket; Fl, flagellum; G, Golgi; M, mitochondria; N, nucleus; A, acidocalcisome.



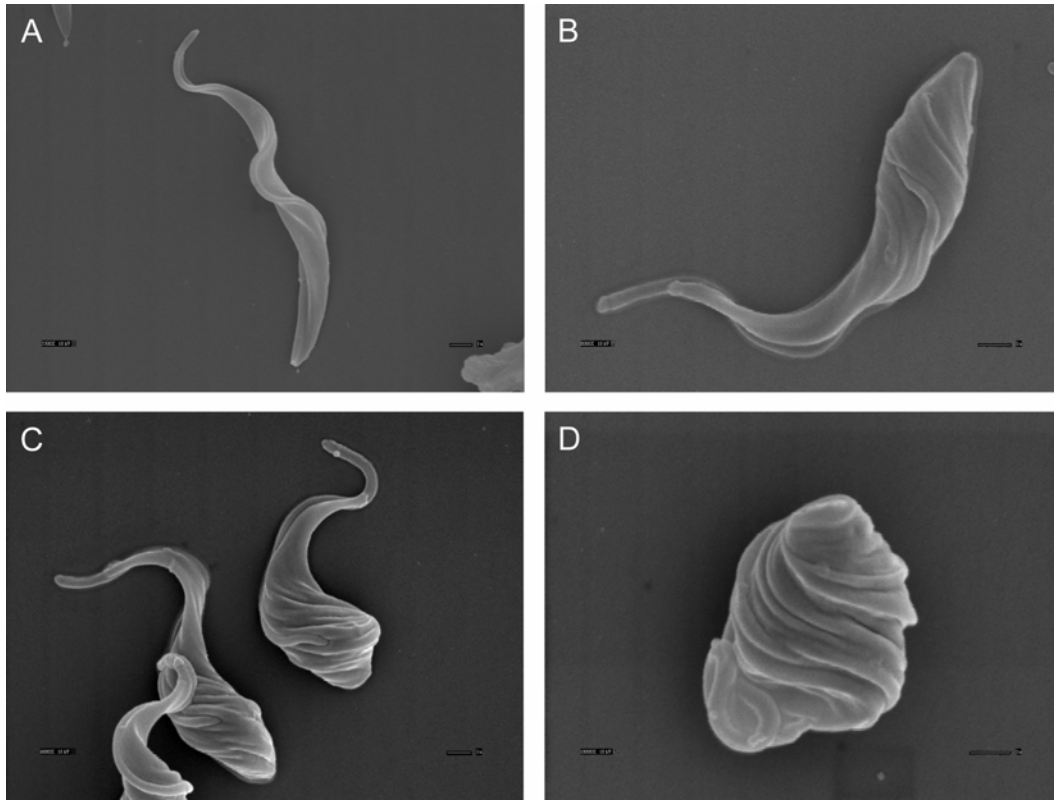


Figure 4.4. Cells depleted of TbPI4KIII- $\beta$  have an abnormal twisted shape. Scanning electron microscopy revealed an abnormal twisted phenotype in cells induced for six days (B-D), compared to uninduced cells (A). Magnification: (A) 5500x, (B) 8000x, (C) 6000x, (D) 10000x. Scale bars: 1  $\mu$ m.

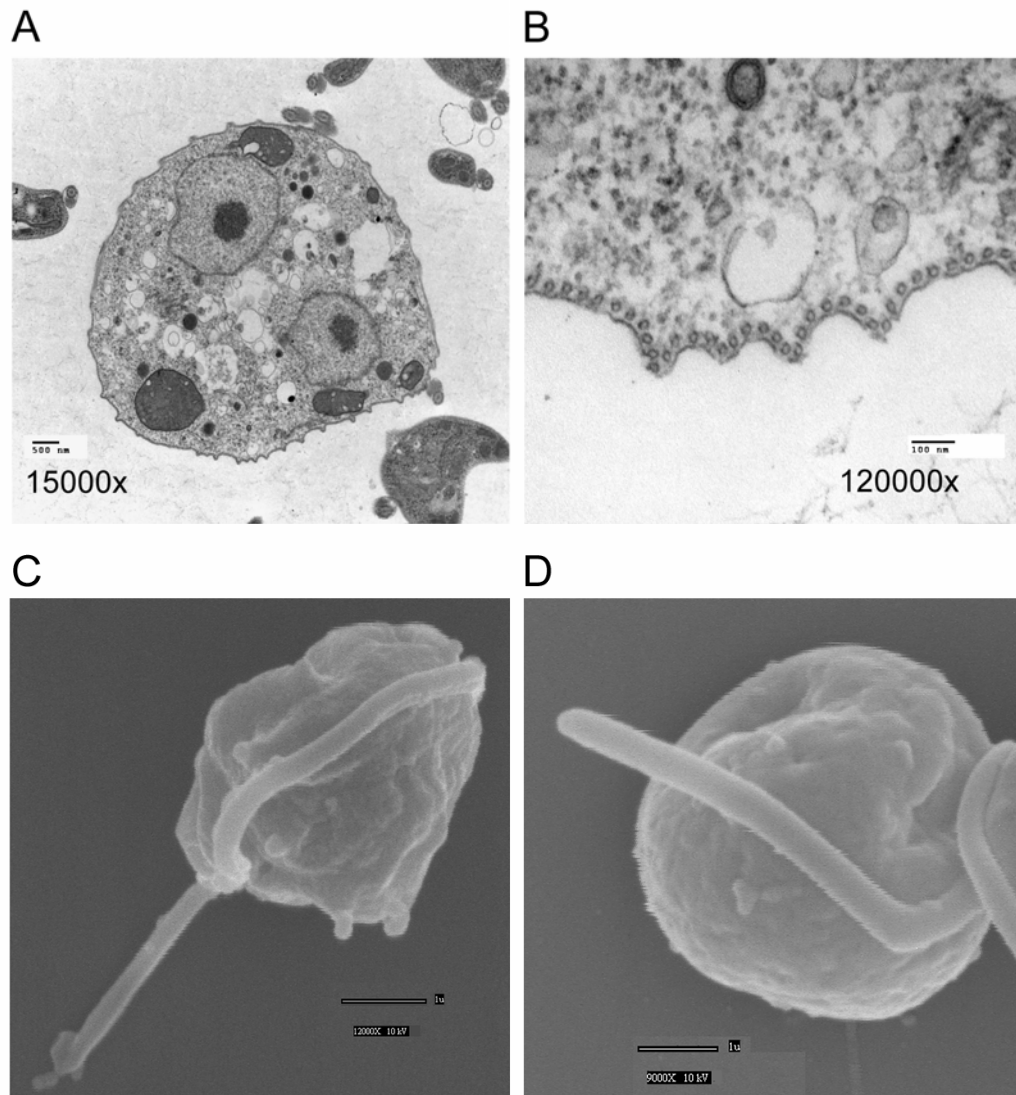


Figure 4.5. Cells depleted of TbPI4KIII- $\beta$  eventually collapse. A subpopulation of induced cells displayed abnormal membrane structure and appeared to be in the process of collapsing. TEM images reveal perturbations in the membrane (A-B). TEM scale bar: 500 nm. SEM images reveal protrusions and indentations in the surface (C-D). SEM magnifications: (A) 12000x, (D) 9000x. SEM scale bars: 1  $\mu$ m.

## CHAPTER FIVE

### TbPI4KIII- $\beta$ is Required for Normal Golgi Structure and Function

#### A. Introduction

*T. brucei* have a highly polarized exocytotic and endocytotic system, located between the nucleus and a specialized organelle called the flagellar pocket. This invagination of the plasma membrane near the posterior of the cell is the only site of exocytosis and endocytosis. (Gull 2003). Both forms of the parasite express a stage-specific GPI-anchored surface protein (Cross 1975; Stebeck and Pearson 1994). The bloodstream form parasites are able to undergo antigenic variation by switching the expression of their variable surface glycoproteins (VSG), thereby evading the human immune response (Pays, Vanhamme et al. 1994). Procyclic form parasites express two isoforms of the procyclic acidic repetitive protein procyclin, which is believed to protect the parasite from harsh environment of the fly midgut (Gruszynski, van Deursen et al. 2006). Surface coat proteins comprise the bulk of protein cargo moving through the secretory system (Field and Carrington 2004). Bloodstream form parasites also have a high rate of VGS endocytosis and recycling at the flagellar pocket (FP). This process is also important for immune evasion allowing for degradation of bound host immune complexes. Endocytosis at the FP is important in both forms for uptake of nutrients and for host-parasite interactions. Trafficking, endocytosis and Golgi maintenance are all phosphoinositide-mediated events in other eukaryotes (Field and Carrington 2004). Many of the components of the exocytotic and endocytotic systems in have been identified,

including clathrin, adapter-proteins and Rab GTPases (Field and Carrington 2004), some of which are known effector proteins of D4 phosphorylated PIs in other eukaryotes. This suggest that the synthesis D4 phosphorylated PIs may play a key regulatory role the secretory pathway in *T. brucei*.

## **B. Materials and Methods**

### **1. Cell Culture**

The TbPI4KIII- $\beta$  RNAi cell cultures were grown at 25°C in SDM-79 supplemented with 10% FBS, in the presence of 25  $\mu$ g/ml G418, 25  $\mu$ g/ml hygromycin and 2.5  $\mu$ g/ml phleomycin. Synthesis of RNA was induced by the addition of tetracycline at 1  $\mu$ g/ml (Wang, Morris et al. 2000). RNAi induced cultures were continually cultured in the presence of tetracycline and were split when necessary.

### **2. Immunofluorescence Microscopy**

Cells for Immunofluorescence were washed once with PBS and adhered to poly-L-lysine coated slides. Cells were fixed with 3.7 % Formaldehyde (EMS) in PBS for 30 min at room temperature. Cells were washed three times with PBS and permeablized with 0.1% Triton X-100/PBS for 10 minutes. Cells were washed three times with 1% normal goat serum (NGS)/PBS and blocked for 1hr with 10% NGS/PBS, followed by incubation with the first primary antibody in 10% NGS/PBS for 1hr at room temperature. Dual stained cells were washed three times with 1% NGS/PBS, followed by incubation with the second primary antibody in 10% NGS/PBS for 1hr at room temperature. Primary antibody dilutions are as follows: rabbit anti-TbBip, 1:1000 (Bangs, Uyetake et

al. 1993), mouse anti-p67, 1:500 (Kelley, Alexander et al. 1999), rabbit anti-Trypanopain, (Troeborg, Pike et al. 1997), and rabbit anti-CRAM, 1:300 (Lee, Bihain et al. 1990). Following incubation with primary antibody(s), cells were washed three times with 1% NGS/PBS and incubated with Dylight560 labeled goat anti-rabbit IgG (Pierce) in 10% NGS/PBS for 1 hr at room temperature. Dual stained cells were then incubated with AlexaFluor488 labeled goat anti-mouse IgG (Molecular Probes) in 10% NGS/PBS for 1 hr at room temperature. Secondary antibody dilutions are as follows: Dylight560 labeled goat anti-rabbit IgG (Pierce) 1:200 and AlexaFluor488 labeled goat anti-mouse IgG (Molecular Probes) 1:200. To visualize the Golgi cells were fixed and permeablized with ice cold 100% methanol for 5 minutes and then washed three times with 3% BSA in PBS. Cells were then blocked for 1 hr with 3% BSA/PBS and then incubated with rabbit anti-TbGrasp antibody 1:500 (He, Ho et al. 2004) in 3% BSA/PBS for 1hr at room temperature followed by incubation of with mouse anti-p67, 1:500 (Kelley, Alexander et al. 1999). Cell were washed three times with 3%BSA/PBS and incubated with Dylight560 labeled goat anti-rabbit IgG (Pierce) 1:200, in 3%BSA/PBS for 1 hr at room temperature, followed by incubation with AlexaFluor488 labeled goat anti-mouse IgG (Molecular Probes) 1:200, in 3%BSA/PBS for 1 hr at room temperature. All slides were mounted in vectashield mounting media containing DAPI (Vector Labs) in order to stain the kinetoplast and nucleus. All fluorescence microscopy was performed with a Zeiss Axiovert 200M inverted microscope equipped with a Zeiss 100x numerical aperture oil immersion objective, and a CCD camera. Digital images were captured and analyzed using Slidebook 4.0 software (Intelligent Imaging Innovations) and images prepared with Adobe Photoshop (5.5).

### 3. Transmission Electron Microscopy

Cells for transmission electron microscopy were fixed in suspension by adding 5% glutaraldehyde and 6.4% paraformaldehyde in PBS to trypanosomes in an equal volume of growth medium. Cells were then rinsed, pelleted, and embedded in 2% agarose. Small pieces of cell pellet were post-fixed with 1% osmium tetroxide, dehydrated in a graded ethanol series, and embedded in EMbed-812 resin. Thin-sections were cut on a LEICA EM UC6 ultramicrotome, post-stained with uranyl acetate and lead citrate, and viewed in a JEOL JEM-1200EX electron microscope operating at 80 kV.

## C. Results

### 1. TbPI4KIII-b is Required for the Correct Localization of Protein markers

PI4KIII- $\beta$  plays a major role in Golgi maintenance and secretion in other organisms. Ultrastructural analysis of TbPI4KIII- $\beta$  depleted cells indicated a possible defect at the Golgi. We used immunofluorescence microscopy to further explore the abnormal phenotype seen in cells depleted of TbPI4KIII- $\beta$ . Initially we examined the localization of a marker for the ER, TbBip (Bangs, Uyetake et al. 1993). *T. brucei* have an extensive ER, which extends throughout the cytoplasm (Fig 5.1-A). A similar pattern is seen in the induced cells, indicating that the ER in these cells is relatively normal (Fig 5.1-B). We used TbGRASP as a marker for the Golgi (He, Ho et al. 2004). In uninduced cells (Fig 5.2-A), TbGRASP stains a single Golgi structure located between the nucleus and the kinetoplast. Cells depleted of TbPI4KIII- $\beta$  displayed an abnormal staining pattern. In these cells, TbGRASP, stained multiple punctuate structures and there was an

increase in background staining (Fig 5.2-A), indicating that cells depleted of TbPI4KIII- $\beta$  have a defect in the Golgi structure. We also wanted to examine the localization of markers for the lysosome and the flagellar pocket. We used p67 as a marker for the lysosome. p67 is a type I membrane protein, which localizes to the lysosome (Kelley, Alexander et al. 1999). In uninduced cells, p67 stains a region between the kinetoplast and the nucleus (Fig 5.2-A & B). After induction p67 was no longer localized to one region, but stained several punctuate regions throughout the cytoplasm. Similar to the TbGRASP staining there was an increase in background staining. We used the CRAM protein as a marker for the flagellar pocket. CRAM is a highly expressed type I transmembrane protein in procyclic cells. It is a putative lipoprotein receptor, which localizes to the FP (Lee, Bihain et al. 1990). Typically CRAM stains one or two structures in the posterior region of the cell, near the kinetoplast (Fig.5.2-B). TbPI4KIII- $\beta$  depleted cells displayed an abnormal staining pattern. CRAM was mislocalized throughout the cytoplasm, with diffuse staining and staining of multiple punctuate structures (Fig.5.2-B). This indicates that CRAM is no longer localized to the flagellar pocket. Both CRAM and p67 are distributed throughout the cytoplasm in the TbPI4KIII- $\beta$  depleted cells, but CRAM displays a much more extreme phenotype, with intense staining throughout the cytoplasm (Fig 5.2-B). We also examined the localization of another lysosomal protein, trypanopain, which is a soluble cysteine protease (Troeborg, Pike et al. 1997). The normal trypanopain staining pattern (Fig 5.3-A), is similar to what is seen with p67, staining one or two structures between the nucleus and the kinetoplast (Fig 5.2-A-B). The induced cells had an abnormal staining pattern similar to the CRAM staining, although trypanopain does not appear to be localized to membrane bound

vesicles. The abnormal staining of all the markers examined indicates that depletion of TbPI4KIII- $\beta$  causes a defect at the Golgi.

#### **D. Discussion**

It is well known that synthesis of PI4P at the Golgi is important for maintenance of the structural and functional organization of the Golgi (De Matteis, Di Campli et al. 2005). Loss of PI4KIII- $\beta$  in other organisms results in morphological defects in the Golgi apparatus and defects in the secretory pathway (Balla and Balla 2006). Immunofluorescence analysis in TbPI4KIII- $\beta$  depleted cells reveals mislocalization of the Golgi marker and markers for the lysosome and flagellar pocket. The ER was relatively normal in the RNAi cells, having the characteristic reticulated staining pattern seen in normal cells. The abnormal staining patterns seen with TbGrasp, p67, CRAM and trypanopain, do not have the reticular staining pattern of the ER, indicating they are not being retained in the ER. Normally proteins destined for the Golgi or the secretory pathway leave the ER and enter the Golgi. TbGrasp, p67 and CRAM predominantly localize to what appear to be membrane bound vesicles throughout the cytoplasm. Trypanopain localizes throughout the cytoplasm and does not appear to be contained in vesicles. TEM analysis also reveals a heterogeneous population of vesicles throughout the cytoplasm. The abnormal membrane bound structures may be vesicle intermediates, which originate from affected organelles, such as the ER, Golgi, or the endosomes. Ablation of clathrin heavy chain in procyclic results in similar morphological abnormalities, including rounded shape, accumulation of cytoplasmic vesicles and mislocalization of CRAM (Allen, Goulding et al. 2003). In mammalian cells, the



clathrin adapter protein AP-1 is recruited to the TGN by a pool of PI4P synthesized by PI4KII- $\alpha$  (Wang, Wang et al. 2003). Because *T. brucei* lack the Type II isoforms, it is likely that this function in *T. brucei* is performed by TbPI4KIII- $\beta$ . Trafficking of CRAM to the FP, but not p67 to the lysosome or EP to the surface, is clathrin-dependent in procyclic (Hung, Qiao et al. 2004). Loss of PI4P synthesis causes a more global defect in secretion and the Golgi, affecting trafficking to the lysosome, in addition to flagellar pocket transport.

Synthesis of PI4P by PI4KIII- $\beta$  at the Golgi is important for lipid transport in other eukaryotes (Balla and Balla 2006). Synthesis of sphingomyelin from ceramide in the Golgi, requires CERT (ceramide transfer protein)-dependent transfer of ceramide from the ER (Toth, Balla et al. 2006). Sphingomyelin, along with cholesterol, are components of lipid rafts, which are lipid microdomains important for protein sorting and signal transduction (Mayor and Rao 2004). CERT is localized to the Golgi membrane through its PH domain, which binds specifically to PI4P. Oxysterol-binding proteins (OSBPs) also bind specifically to PI4P through their PH domains. OSBP localizes to the Golgi apparatus in response to oxysterols, this interaction is PI4P and Arf1-dependent (Lagace, Byers et al. 1997; Levine and Munro 1998; Godi, Di Campli et al. 2004). Localization to the Golgi activates CERT-dependent transport of ceramide to the Golgi, thereby integrating sterol homeostasis and SM synthesis (Perry and Ridgway 2006). Procyclic *T. brucei* are able to synthesize ergosterol, but also use exogenous LDL as a source of cholesterol and lipids (Coppens and Courtoy 1995). The major complex sphingolipid synthesized in *Leishmania* sp. and *Trypanosoma* sp. is inositol phosphorylceramide (IPC) (Lester and Dickson 1993). Unlike mammalian cell, which

synthesize SM from ceramide, *T. brucei* acquire theirs from LDL, which can be degraded to provide components for the synthesis of phosphatidylcholine, triacylglycerols, and cholesteryl esters (Coppens and Courtoy 1995). Inhibition of sterol biosynthesis in *Leishmania amazonensis* causes a similar alteration of membrane bound compartments as seen with depletion of TbPI4KIII- $\beta$  (Vannier-Santos, Martiny et al. 1999). Inhibition of HMG-CoA reductase in procyclic *T. brucei* also results in a cytokinesis block and in the accumulation of abnormal membrane compartments (Coppens and Courtoy 1995). The similarities with the morphological defects in PI4P depleted cells, indicate that loss of TbPI4KIII- $\beta$  may affect lipid homeostasis in addition to its affects on the secretory pathway.

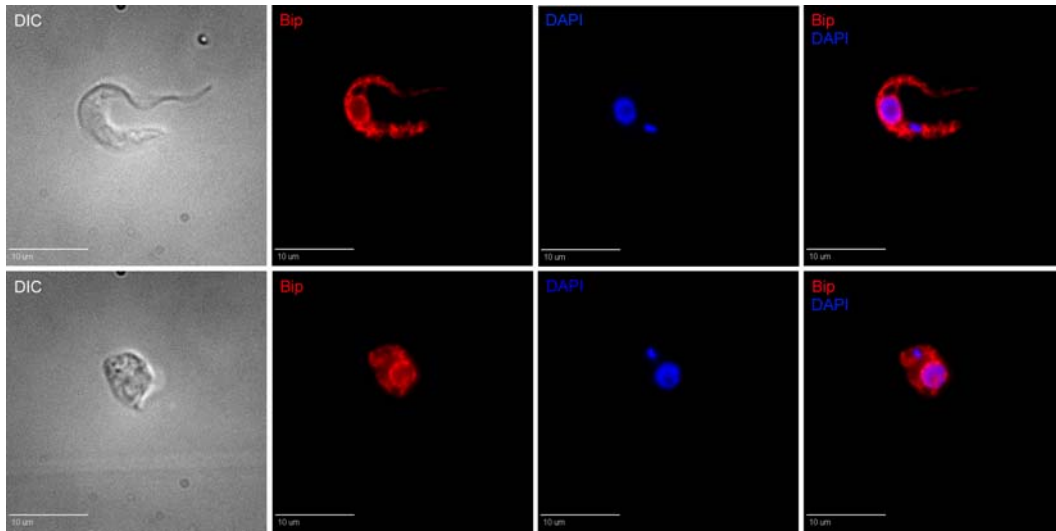


Figure 5.1. Depletion of TbPI4KIII- $\beta$  does not affect the ER. TbBip (Red) was used to visualize the ER. The kinetoplast and the nucleus were stained with (DAPI). TbBIP staining produces a reticular staining pattern (A). In cells induced for six days, the staining pattern appeared normal (B).

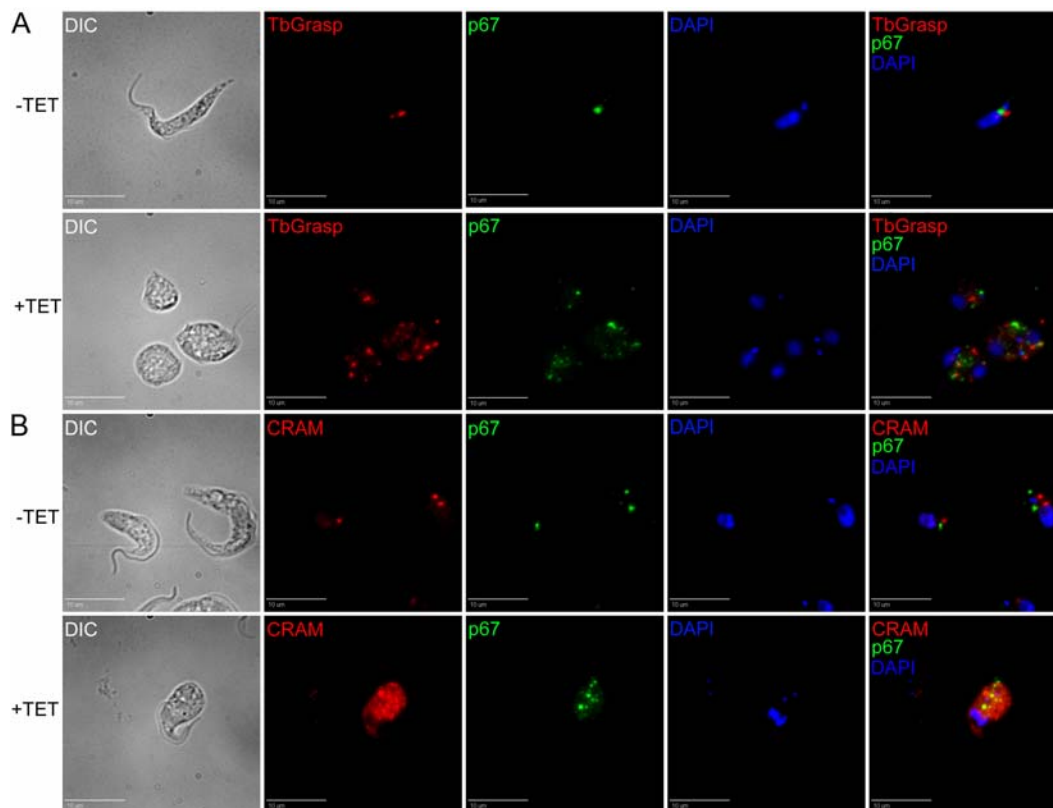


Figure 5.2. Abnormal localization of protein markers for the Golgi, lysosome and flagellar pocket in cells depleted of TbPI4KIII- $\beta$ . Immunofluorescence analysis of markers for the Golgi, TbGrasp (Red) and lysosome, p67 (Green) (A) and the flagellar pocket, CRAM and lysosome, p67 (Green) (B). The kinetoplast and nucleus was stained with DAPI (Blue). Cells depleted of TbPI4KIII- $\beta$  displayed an abnormal staining pattern for all markers examined (A and B), indicating a defect at the Golgi. +TET cells were induced for six days. Scale bars: 10  $\mu$ m.

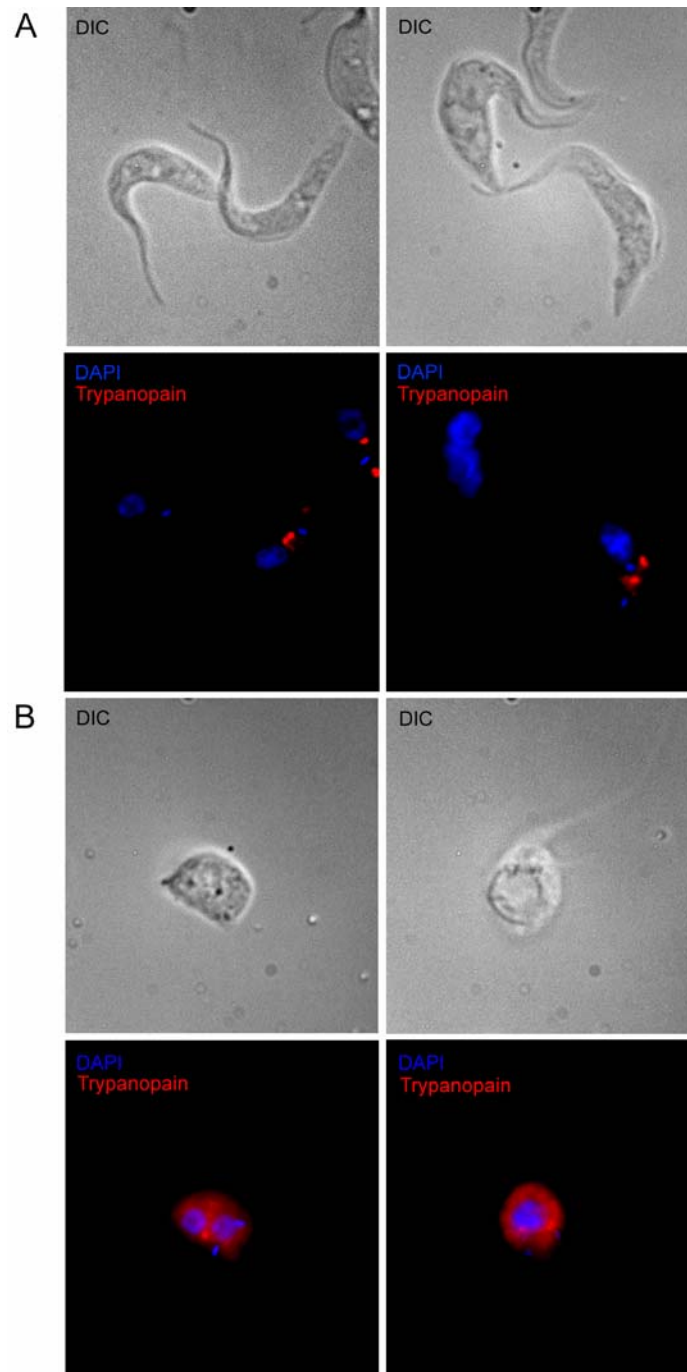


Figure 5.3. Abnormal localization of the lysosomal marker trypanopain in cells depleted of TbPI4KIII-β. Immunofluorescence analysis of the lysosomal marker trypanopain in

uninduced cells (A) and cells induced for six days (B). Depletion of TbPI4KIII- $\beta$  caused trypanopain to be mislocalized throughout the cytoplasm (B).



## CHAPTER SIX

### **TbPI4KIII- $\beta$ is Required for Cytokinesis in Procyclic Form *T. brucei***

#### **A. Introduction**

In addition to the nuclear mitotic events normally seen in eukaryotic cell division, *T. brucei* must coordinate the duplication and segregation of the mitochondrial genome, which comprises a specialized organelle known as the kinetoplast ((Sherwin and Gull 1989). The timing of kinetoplast and nuclear DNA division, and other morphological events in procyclic have been elucidated (Woodward and Gull 1990). The first morphological events in the cell cycle are the formation of the pro-basal body and nucleation of the daughter flagellum (Fig. 6.1) (McKean, Baines et al. 2003). Kinetoplast and nuclear DNA S phase begin at around the same time, but the kinetoplast replication and segregation cycle is much shorter than the nuclear cycle. Kinetoplast duplication and segregation are completed before the onset of nuclear mitosis (Fig. 6.1) (Woodward and Gull 1990). The basal body of *T. brucei* is physically attached to the kinetoplast through the tripartate attachment region, which extends through both the cell and mitochondrial membranes (Ogbadoyi, Robinson et al. 2003), and segregates with the kinetoplast (Woodward and Gull 1990). During the elongation of the daughter flagellum, its distal tip is physically attached to the old flagellum. This attachment is believed to provide a directional cue for growth of the new flagellum (Moreira-Leite, Sherwin et al. 2001). The flagellum is attached to the cell body through a specialized structure called the flagellar attachment zone (FAZ) (Sherwin and Gull 1989; Kohl, Sherwin et al. 1999). Outgrowth and attachment of the new flagellum also defines the site of the cleavage



furrow, which initially forms at the anterior end of the parasite and ingresses between the two flagella (McKean, Baines et al. 2003). Depletion of one of the protein components of the FAZ, flagellum adhesion glycoprotein 1 (FLA1), results in a defect in cytokinesis, indicating that a properly formed FAZ is required for cytokinesis (Moreira-Leite, Sherwin et al. 2001; LaCount, Barrett et al. 2002).

Procyclic *T. brucei* are unique in that progression through cytokinesis is not dependent on nuclear mitosis or DNA synthesis, indicating that this life stage lacks the mitosis to cytokinesis checkpoints. Cells blocked in mitosis will proceed through cytokinesis resulting in anucleated cells known as zoids (Ploubidou, Robinson et al. 1999; Hammarton, Clark et al. 2003; Li and Wang 2003). It is postulated that it is kinetoplast-basal body segregation that drives cytokinesis in these cells (Ploubidou, Robinson et al. 1999). Inhibition of the kinetoplast segregation cycle with okadaic acid results a block in cytokinesis, but mitosis is not affected (Das, Gale et al. 1994).

Depletion of TbPI4KIII- $\beta$  in procyclic cells caused a block in cytokinesis. These cells appear to progress through kinetoplast duplication and segregation, and mitosis. The cells often had a detached flagellum and lacked a visible cleavage. These results indicate that TbPI4KIII- $\beta$  is required for cytokinesis, possibly acting directly at the cleavage furrow.

## **B. Materials and Methods**

### **1. Cell Culture**

The TbPI4KIII- $\beta$  RNAi cell cultures were grown at 25°C in SDM-79 supplemented with 10% FBS, in the presence of 25  $\mu$ g/ml G418, 25  $\mu$ g/ml hygromycin

and 2.5 µg/ml phleomycin. Synthesis of RNA was induced by the addition of tetracycline at 1 µg/ml (Wang, Morris et al. 2000). RNAi induced cultures were continually cultured in the presence of tetracycline and were split when necessary.

## **2. Immunofluorescence**

Immunofluorescence microscopy was performed as described previously in Chapter 5. Briefly, cells were fixed with 3.7 % Formaldehyde (EMS) in PBS and permeablized with 0.1% Triton X-100/PBS for 10. They were then blocked for 1hr with 10% NGS in PBS, followed by incubation with the primary antibody, rat-anti YL1/2, 1:500 (Chemicon), in 10% NGS/PBS for 1hr at room temperature. YL1/2 is a monoclonal antibody for tyrosinated tubulin, which has presiously been shown to stain for the basal body in *T. Brucei* (Sherwin and Gull 1989). Cells were then incubated with Dylight560 labeled goat anti-rabbit IgG (Pierce) in 10% NGS/PBS for 1 hr at room temperature. Slides were mounted in Vectashield mounting media containing DAPI (Vector Labs).

## **3. Analysis of DNA Content**

Log phase cells from both uninduced and induced cells were collected over a six day period.  $2 \times 10^7$  trypanosomes were collected and washed once with PBS. Pellets were resuspended in 1.0 ml PBS and adhered to poly-L-lysine coated slides. Cells were fixed for 5 min in ice-cold 100% methanol and washed with PBS. Slides were then mounted in Vectashield mounting media containing DAPI (Vector Labs).

Individual cells were examined with a fluorescence microscope, in order to determine the percentage of cells in different phases of the cell cycle. A population of one hundred cells for each day in uninduced and induced cells was counted and four different cell cycle phenotypes were scored. The four phenotypes correspond to kinetoplast and nuclear content. The first phenotype, which corresponds to G1, has 1 kinetoplast and 1 nucleus. The second phenotype has 2 kinetoplasts and 1 nucleus. The third phenotype, which has 2 kinetoplasts and 2 nuclei, corresponds to cells in G2/M. The fourth phenotype corresponded to any other combination of kinetoplast and nuclear content. The counts from three independent experiments were averaged and the standard deviation was calculated.

#### **4. Scanning Electron Microscopy**

Methods for SEM are described in Chapter 2.

### **C. Results**

#### **1. Effect of TbPI4III- $\beta$ Depletion on Cell Cycle Progression in Procytic Form *T. brucei***

In order to determine the effect of TbPI4III- $\beta$  depletion on cell cycle progression, the kinetoplast and nuclear content of uninduced and induced cells was calculated in DAPI stained cells. The percentage of cells, in four different stages of the cell cycle, was calculated from a population of one hundred cells for each sample. Analysis of the uninduced cells, in log phase growth, revealed that approximately 65% of the cells were in G1 and approximately 15-20% of the cells were in G2/M at all times examined. After

5 days of tetracycline induction (Fig. 6.2-B), the percentage of cells in G1 decreased from 68%, in uninduced cells, to 43%. The percentage of cells in G2/M increased from 16%, in uninduced cells, to 31%. By six days of induction the percentage of cells in G1 had decreased to 33% and the percentage of cell in G2/M had increased to 45 % of the cells. There were a few cells with abnormal DNA content found both uninduced and induced cultures, but depletion of TbPI4KIII- $\beta$  did not result in an increase in the number of anucleated cells (zoids) or in cells with DNA content greater than 2K2N. Cells depleted of TbPI4KIII- $\beta$  replicate both the kinetoplast and the nucleus, but are blocked at cytokinesis. These cells do not continue to replicate their DNA following the cytokinesis block.

## **2. Effect of TbPI4KIII- $\beta$ Depletion on Kinetoplast and Nuclear Segregation**

In order to investigate further the effects of depletion of TbPI4KIII- $\beta$  on the cell cycle, we followed kinetoplast segregation and nuclear division throughout the cell cycle (Fig-6.3). Uninduced and induced cells were stained with DAPI, to stain the kinetoplast and the nucleus, and YL1/2, which stains the basal body. The basal body of *T. brucei* is physically attached to the kinetoplast through the tripartate attachment region, which extends through both the cell and mitochondrial membranes (Ogbadoyi, Robinson et al. 2003). Elongation and maturation of the pro basal body and nucleation of the new flagellum are the first events in the cell cycle of *T. brucei* (McKean, Baines et al. 2003). Kinetoplast replication and division occur soon after, followed by nuclear division (Woodward and Gull 1990). Depletion of TbPI4KIII- $\beta$  does not effect duplication of the

basal bodies or the kinetoplasts. Both the basal body and kinetoplast duplicate and segregate together (Fig 6.3-B), although the direction of segregation is abnormal. The new basal body/kinetoplast is usually positioned posterior to the old basal body/kinetoplast (Fig. 6.3-A). As the cell cycle progresses the new basal body/ kinetoplast moves toward the posterior end of the cell (Fig 6.3-A). During mitosis the daughter nucleus moves towards the posterior so that eventually the cell has the characteristic 2K2N configuration, with the old basal body/kinetoplast between the two nuclei (Fig 6.3-A). The induced cells no longer maintain this strict spatial organization (Fig 6.3-B). The basal bodies/kinetoplasts segregate perpendicular to the normal anterior to posterior directional axis (Fig 6.3-B). Nuclear division proceeds at the appropriate time, although the positioning of the kinetoplasts and nuclei are abnormal in the induced cells (Fig 6.3B). These cells do not have characteristic 2K2N configuration, with the old basal body/kinetoplast between the two nuclei (Fig 6.3-A).

### **3. Dividing TbPI4KIII- $\beta$ depleted cells lack a cleavage furrow**

Scanning electron microscopy was utilized to examine the abnormal morphology of TbPI4KIII- $\beta$  depleted cells. As discussed previously, these cells had an abnormal twisted morphology, which became more severe over time. Dividing cells were easily identifiable by the presence of two flagella (Fig 6.4). Although these cultures contained many cells in the process of dividing, an obvious cleavage furrow was not identified in these cells. The cleavage furrow can be easily identified in the uninduced cultures (Fig. 6.4-A). The cleavage furrow usually begins at the anterior, between the two flagellum,

and moves towards the posterior end. It was also noted that many of the dividing cells had a detached daughter flagellum (Fig. 6.4-B).

#### **D. Discussion**

Depletion of TbPI4KIII- $\beta$  by RNAi in procyclic *T. brucei* resulted in the accumulation of cells in G2/M, which indicated that TbPI4KIII- $\beta$  is required for cytokinesis in these cells. These cells underwent a single round of mitosis, but were not able to correctly position the kinetoplasts or the nuclei. These cells also lacked a visible cleavage furrow and often had a detached daughter flagellum.

The cytokinesis block observed in TbPI4KIII- $\beta$  depleted cells may be caused directly by depletion of phosphoinositides at the site of the cleavage furrow. Phosphoinositides are implicated in the coordination of membrane and cortical actin events during cytokinesis in other organisms (Janetopoulos and Devreotes 2006). In other organisms, PI4KIII- $\beta$  has been shown to be required for cytokinesis. Mutations in the gene for PI4KIII- $\beta$  in *Drosopholia melanogaster*, known as four wheel drive (fwd), causes a defect in cytokinesis during male meiosis (Brill, Hime et al. 2000). Temperature sensitive mutant alleles in the *Schizosaccharomyces ceravesiae* homolog pik1, are also defective in cytokinesis (Garcia-Bustos, Marini et al. 1994; Walch-Solimena and Novick 1999). This enzyme is also required for cytokinesis in *Schizosaccharomyces pombe*. In these cells, PI4KIII- $\beta$  interacts with the contractile ring protein Cdc4p and is most likely responsible for the recruitment and/or assembly of some of the many proteins required for the formation and/or function of the contractile ring

(Desautels, Den Haese et al. 2001). Exactly how the cleavage furrow forms and ingresses in *T. brucei* is not known at this time. It is known that cleavage does not involve an actin/myosin II contractile ring at the cleavage furrow (Dutcher, Huang et al. 1984). Currently, there are no protein markers for the cleavage furrow in *T. brucei*, so localization studies are not possible.

Correct positioning of cytoskeletal elements and organelles is important for the progression through the cell cycle and cytokinesis (McKean, Baines et al. 2003). The induced cells go through mitosis, but positioning of the kinetoplast and nucleus are abnormal. After nuclear division, the daughter kinetoplast and nucleus segregate towards the posterior of the cell, resulting in one kinetoplast between the two nuclei (Sherwin and Gull 1989). In the TbPI4KIII- $\beta$  RNAi cells, the kinetoplasts and the nuclei often segregate perpendicular to the normal lengthwise axis. Cells depleted of TbPI4KIII- $\beta$  often exhibited a detached daughter flagellum, which indicates a possible abnormality in the flagellar attachment zone (FAZ). Correct positioning of the daughter flagellum and/or the FAZ is important for the cleavage furrow (Gull 2003). The loss of these structural cues may be responsible for the block in cytokinesis.

*T. brucei* do not have a mitosis to cytokinesis checkpoint and are therefore able to proceed with cytokinesis in the absence of mitosis (Ploubidou, Robinson et al. 1999). Another unusual feature of *T. brucei* is their ability to reinitiate DNA synthesis and mitosis in the absence of cytokinesis. Cells depleted of TbPI4KIII- $\beta$  are unusual in that although cytokinesis is blocked, their DNA does not continue to duplicate. Depletion of TbPI4KIII- $\beta$  may have activated a cell cycle checkpoint, thereby preventing continued

synthesis of DNA. It is possible that mitosis is not truly completed in these cells and therefore synthesis is not reinitiated and cytokinesis does not proceed.



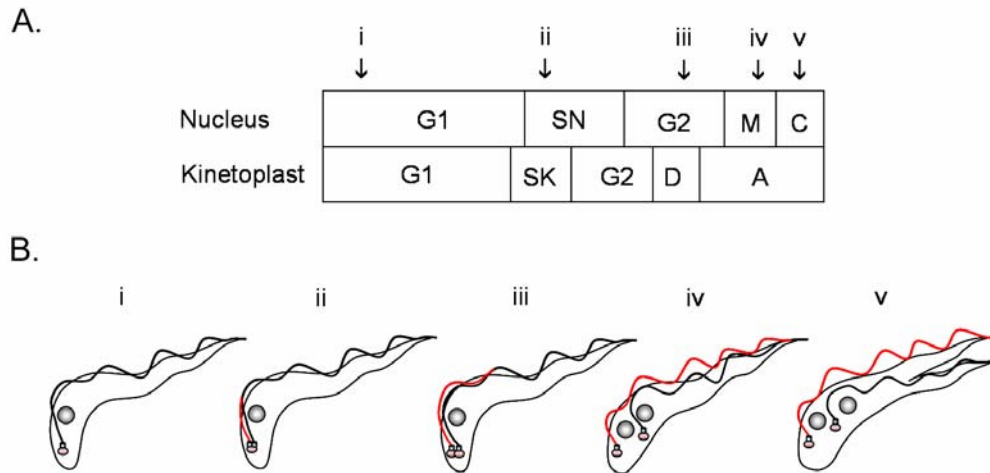
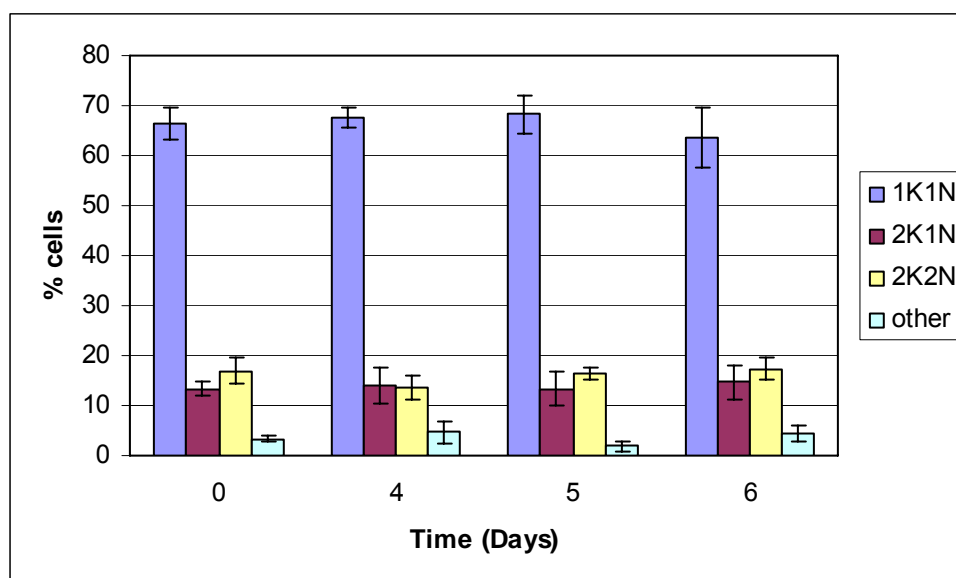


Figure 6.1. Procyclic *T. brucei* cell cycle. (A) The *T. brucei* cell cycle consists of a nuclear and kinetoplast cycle. Kinetoplast replication (SK) begins immediately before nuclear S phase (SN) and is shorter. Kinetoplast segregation (D) is completed before the onset of mitosis (M). During what is known as the apportioning phase (A), the basal bodies continue to move apart. (B) The major morphological events of the cell cycle are represented. The first morphological change is the duplication of the basal body and nucleation of the new flagellum (ii), followed by duplication of the kinetoplast (iii). The kinetoplasts segregate after nuclear S phase (iv), followed by mitosis and cytokinesis (v) (Woodward and Gull 1990).

A.



B.

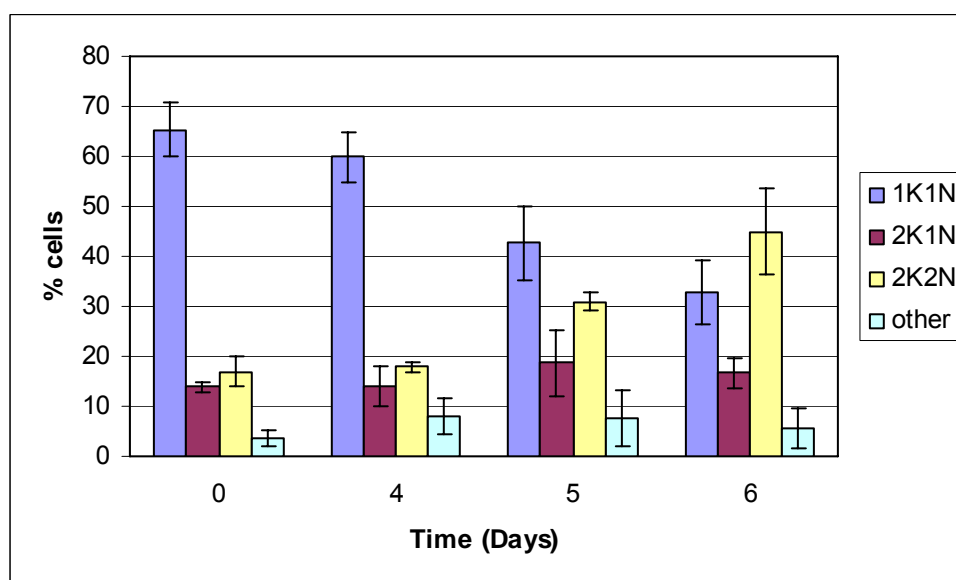


Figure 6.2. Cell cycle analysis of procyclic form TbPI4KIII- $\beta$  RNAi cells. The cell cycle was followed in uninduced (A) and induced RNAi cells (B) over time. The number of kinetoplast and nuclei in individual DAPI stained cells were counted at different time points. Three independent experiment were counted and averaged for each day. Error bars represent the standard deviation.

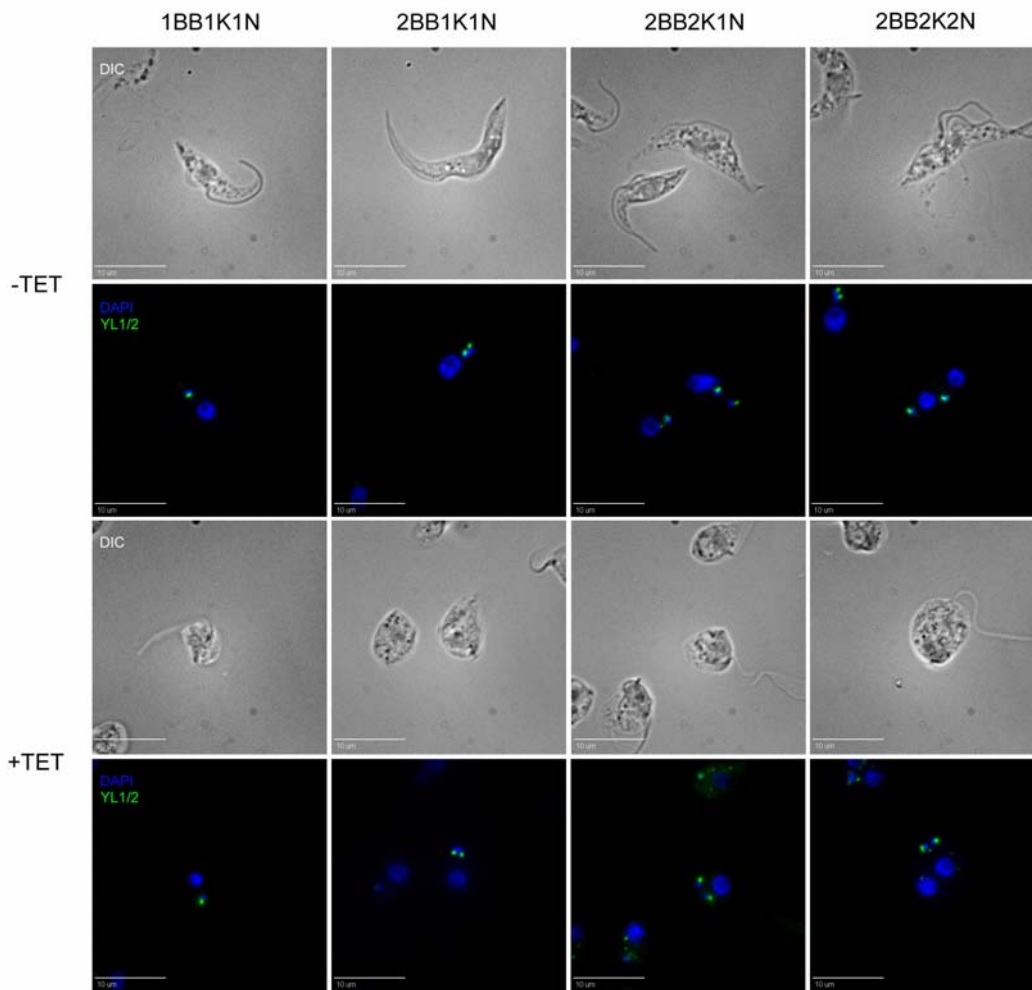


Figure 6.3 Analysis of morphological cell cycle events in procyclic form TbPI4KIII- $\beta$  RNAi cells. The number and position of the basal body, kinetoplast and nucleus were examined by fluorescence microscopy in uninduced cells (-TET) and cells induced for 6 days (+TET). Cells were stained with DAPI (Blue) and YL1/2 (Green), which stains for then basal body.

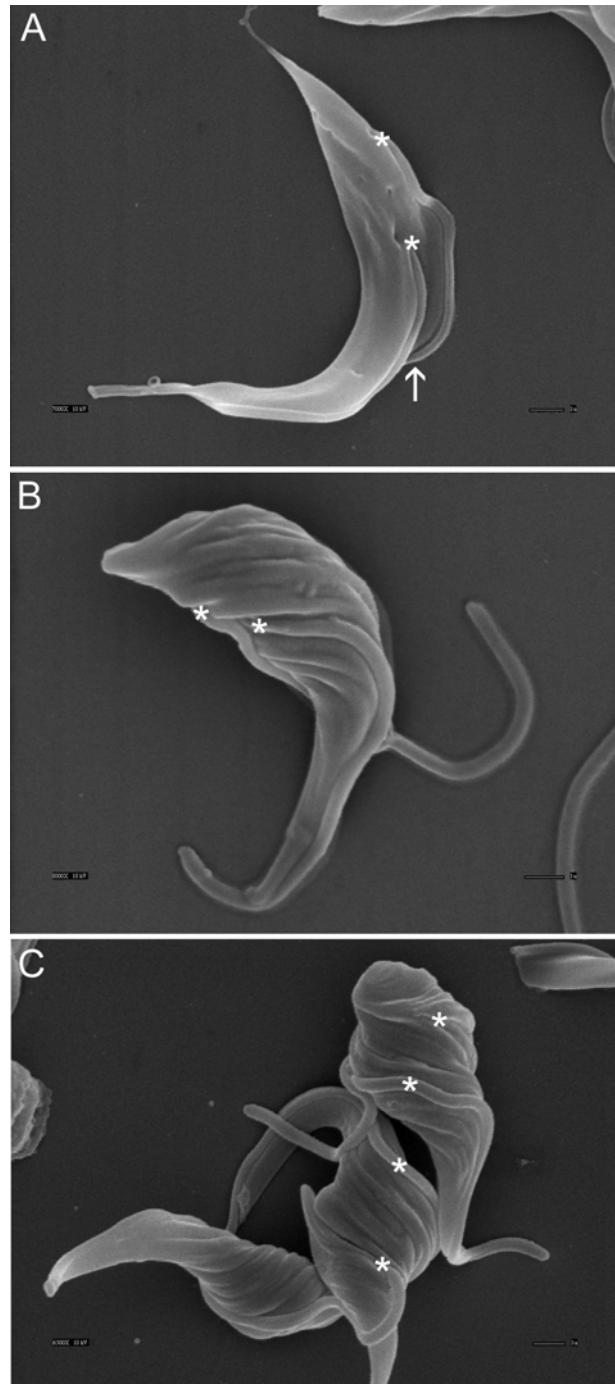


Figure 6.4. Dividing TbPI4KIII- $\beta$  depleted cells lack a cleavage furrow. Scanning electron micrographs of dividing *T. brucei*. Uninduced cells (A) and cells induced for six days (B-C). A dividing cell is identifiable by the presence of two flagella (\*) and a

cleavage furrow (arrow) (A). Dividing cells in induced cells can also be identified by the presence of two flagella (\*) (B-C). Some of these cells have a detached flagellum (B). None of the induced cells had an obvious cleavage furrow (B-C).

## CHAPTER SEVEN

### Conclusion and Future Directions

We initially identified two phosphatidylinositol 4-kinases in *Trypanosoma brucei* database, TbPI4KIII- $\alpha$  and TbPI4KIII- $\beta$ . Northern blot analysis revealed that both enzymes are expressed in the two life forms of the parasite. We cloned the gene encoding the Type III phosphatidylinositol 4-kinase Beta (TbPI4KIII- $\beta$ ) in *Trypanosoma brucei* and verified that it was an authentic PI4-kinase. Depletion of TbPI4KIII- $\beta$  in procyclic *T. brucei* by RNAi results in inhibition of cell growth and a distorted cellular morphology. Further analysis revealed that TbPI4KIII- $\beta$  is required for maintenance of Golgi structure, protein trafficking, normal cellular shape and cytokinesis. Although we did measure PIP levels in the RNAi cells, we were not able to determine the effect on PIP<sub>2</sub> levels. We are not able at this time to say whether the abnormalities we see are due to a decrease in PIP or PIP<sub>2</sub>. *T. brucei* does have a putative Type I PI4P 5-kinase, which in other organisms, synthesizes PI(4,5)P<sub>2</sub> by phosphorylating PI4P at the 5' position (Oude Weernink, Schmidt et al. 2004). RNAi of this protein would help in distinguishing between PIP-mediated events and PI(4,5)P<sub>2</sub>-mediated events.

We used microscopic techniques to try and elucidate the cause of the morphological defects. While microscopy provides a great deal of information, biochemical analysis would help to further our understanding of the mechanism of the defects. Our analysis revealed a defect at the Golgi and it is assumed that the secretory pathway is also affected. Pulse-chase studies following the transport of p67 to the

lysosome or the procyclin coat protein to the surface would confirm a defect in the secretory pathway.

In this study we did not examine the effect of TbPI4KIII- $\beta$  depletion on endocytosis. *T. brucei* must take up nutrients for survival and do so by endocytosing macromolecules from the environment. Ultrastructural analysis revealed some abnormalities at the flagellar pocket, indicating that the endocytotic system may be affected. Radiolabeled lipoproteins could be used to follow receptor-mediated endocytosis in these cells, while fluid-phase markers could be used to look at fluid-phase uptake.

The *T. brucei* PI4KIII- $\beta$  enzyme is much smaller than the other homologs, and lacks some of the conserved sequences, which regulate localization in other organisms. In this study, we did not do a complete biochemical characterization of the enzyme. Further characterization is needed to determine the kinetic parameters of this enzyme and to determine if it has similar  $K_m$  values for its substrates compared to the other PI4KIII- $\beta$  enzymes. We are able to over-express a Flag-tagged version of our enzyme in COS-7, which would allow us to look at localization in these cells. A more detailed examination of the *T. Brucei* database is needed to find homologs to known PI4P and PI(4,5)P<sub>2</sub> effectors. Some have been identified including, Arf1 and AP-1, but more analysis is needed.

We have demonstrated that the *T. brucei* PI4KIII- $\beta$  enzyme is an essential enzyme in the procyclic form of the parasite, but we have not been able to examine its role in the bloodstream form parasite. Although many attempts have been made at

establishing a bloodstream form TbPI4KIII- $\beta$  RNAi cell line, we have not been successful in this endeavor. Although we are not sure why this has not been possible, there is reason to believe that it is just not possible in this form of the parasite. Although we do use inducible promoters, these promoters are still leaky and deletion of some enzymes is extremely lethal in this form of the parasite. This extreme lethality prevents the establishment of the cell line. Due to the inability to establish the bloodstream form cell line, we predict that TbPI4KIII- $\beta$  is an essential protein in the bloodstream form.

Whether or not TbPI4KIII- $\beta$  would make a good drug target is not known at this time, but we do know that the functions affected in the procyclic form are extremely important in the bloodstream form. The possibility does exist, that differences in the *T. brucei* enzyme, compared to the human enzyme, could be exploited for specific inhibition.



## BIBLIOGRAPHY

- Allen, C. L., D. Goulding, et al. (2003). "Clathrin-mediated endocytosis is essential in *Trypanosoma brucei*." Embo J **22**(19): 4991-5002.
- Audhya, A., M. Foti, et al. (2000). "Distinct roles for the yeast phosphatidylinositol 4-kinases, Stt4p and Pik1p, in secretion, cell growth, and organelle membrane dynamics." Mol Biol Cell **11**(8): 2673-89.
- Balla, A. and T. Balla (2006). "Phosphatidylinositol 4-kinases: old enzymes with emerging functions." Trends Cell Biol **16**(7): 351-61.
- Balla, A., G. Tuymetova, et al. (2002). "Characterization of type II phosphatidylinositol 4-kinase isoforms reveals association of the enzymes with endosomal vesicular compartments." J Biol Chem **277**(22): 20041-50.
- Balla, A., G. Tuymetova, et al. (2005). "A plasma membrane pool of phosphatidylinositol 4-phosphate is generated by phosphatidylinositol 4-kinase type-III alpha: studies with the PH domains of the oxysterol binding protein and FAPP1." Mol Biol Cell **16**(3): 1282-95.
- Bangs, J. D., L. Uyetake, et al. (1993). "Molecular cloning and cellular localization of a BiP homologue in *Trypanosoma brucei*. Divergent ER retention signals in a lower eukaryote." J Cell Sci **105** ( Pt 4): 1101-13.
- Barylko, B., S. H. Gerber, et al. (2001). "A novel family of phosphatidylinositol 4-kinases conserved from yeast to humans." J Biol Chem **276**(11): 7705-8.
- Barylko, B., P. Wlodarski, et al. (2002). "Analysis of the catalytic domain of phosphatidylinositol 4-kinase type II." J Biol Chem **277**(46): 44366-75.
- Bastin, P., A. Galvani, et al. (2001). "Genetic interference in protozoa." Res Microbiol **152**(2): 123-9.
- Bravo, J., D. Karathanassis, et al. (2001). "The crystal structure of the PX domain from p40(phox) bound to phosphatidylinositol 3-phosphate." Mol Cell **8**(4): 829-39.
- Brill, J. A., G. R. Hime, et al. (2000). "A phospholipid kinase regulates actin organization and intercellular bridge formation during germline cytokinesis." Development **127**(17): 3855-64.

- Brun, R. and Schonenberger (1979). "Cultivation and in vitro cloning or procyclic culture forms of *Trypanosoma brucei* in a semi-defined medium. Short communication." Acta Trop **36**(3): 289-92.
- Bruns, J. R., M. A. Ellis, et al. (2002). "Multiple roles for phosphatidylinositol 4-kinase in biosynthetic transport in polarized Madin-Darby canine kidney cells." J Biol Chem **277**(3): 2012-8.
- Cantley, L. C. (2002). "The phosphoinositide 3-kinase pathway." Science **296**(5573): 1655-7.
- Clement, S., U. Krause, et al. (2001). "The lipid phosphatase SHIP2 controls insulin sensitivity." Nature **409**(6816): 92-7.
- Coppens, I. and P. J. Courtoy (1995). "Exogenous and endogenous sources of sterols in the culture-adapted procyclic trypomastigotes of *Trypanosoma brucei*." Mol Biochem Parasitol **73**(1-2): 179-88.
- Cross, G. A. (1975). "Identification, purification and properties of clone-specific glycoprotein antigens constituting the surface coat of *Trypanosoma brucei*." Parasitology **71**(3): 393-417.
- Das, A., M. Gale, Jr., et al. (1994). "The protein phosphatase inhibitor okadaic acid induces defects in cytokinesis and organellar genome segregation in *Trypanosoma brucei*." J Cell Sci **107** ( Pt 12): 3477-83.
- de Graaf, P., E. E. Klapisz, et al. (2002). "Nuclear localization of phosphatidylinositol 4-kinase beta." J Cell Sci **115**(Pt 8): 1769-75.
- De Matteis, M. A., A. Di Campli, et al. (2005). "The role of the phosphoinositides at the Golgi complex." Biochim Biophys Acta **1744**(3): 396-405.
- De Matteis, M. A. and A. Godi (2004). "Protein-lipid interactions in membrane trafficking at the Golgi complex." Biochim Biophys Acta **1666**(1-2): 264-74.
- Desautels, M., J. P. Den Haese, et al. (2001). "Cdc4p, a contractile ring protein essential for cytokinesis in *Schizosaccharomyces pombe*, interacts with a phosphatidylinositol 4-kinase." J Biol Chem **276**(8): 5932-42.
- Docampo, R., W. de Souza, et al. (2005). "Acidocalcisomes - conserved from bacteria to man." Nat Rev Microbiol **3**(3): 251-61.

- Downes, C. P., A. Gray, et al. (2005). "Probing phosphoinositide functions in signaling and membrane trafficking." Trends Cell Biol **15**(5): 259-68.
- Dutcher, S. K., B. Huang, et al. (1984). "Genetic dissection of the central pair microtubules of the flagella of *Chlamydomonas reinhardtii*." J Cell Biol **98**(1): 229-36.
- Field, M. C. and M. Carrington (2004). "Intracellular membrane transport systems in *Trypanosoma brucei*." Traffic **5**(12): 905-13.
- Fruman, D. A., R. E. Meyers, et al. (1998). "Phosphoinositide kinases." Annu Rev Biochem **67**: 481-507.
- Garcia-Bustos, J. F., F. Marini, et al. (1994). "PIK1, an essential phosphatidylinositol 4-kinase associated with the yeast nucleus." Embo J **13**(10): 2352-61.
- Gehrmann, T. and L. M. Heilmeyer, Jr. (1998). "Phosphatidylinositol 4-kinases." Eur J Biochem **253**(2): 357-70.
- Gillooly, D. J., I. C. Morrow, et al. (2000). "Localization of phosphatidylinositol 3-phosphate in yeast and mammalian cells." Embo J **19**(17): 4577-88.
- Godi, A., A. Di Campli, et al. (2004). "FAPPs control Golgi-to-cell-surface membrane traffic by binding to ARF and PtdIns(4)P." Nat Cell Biol **6**(5): 393-404.
- Godi, A., P. Pertile, et al. (1999). "ARF mediates recruitment of PtdIns-4-OH kinase-beta and stimulates synthesis of PtdIns(4,5)P<sub>2</sub> on the Golgi complex." Nat Cell Biol **1**(5): 280-7.
- Gruszynski, A. E., F. J. van Deursen, et al. (2006). "Regulation of surface coat exchange by differentiating African trypanosomes." Mol Biochem Parasitol **147**(2): 211-23.
- Gull, K. (2003). "Host-parasite interactions and trypanosome morphogenesis: a flagellar pocketful of goodies." Curr Opin Microbiol **6**(4): 365-70.
- Hall, B. S., C. Gabernet-Castello, et al. (2006). "TbVps34, the trypanosome orthologue of Vps34, is required for Golgi complex segregation." J Biol Chem **281**(37): 27600-12.

- Hama, H., E. A. Schnieders, et al. (1999). "Direct involvement of phosphatidylinositol 4-phosphate in secretion in the yeast *Saccharomyces cerevisiae*." J Biol Chem **274**(48): 34294-300.
- Hammarton, T. C., J. Clark, et al. (2003). "Stage-specific differences in cell cycle control in *Trypanosoma brucei* revealed by RNA interference of a mitotic cyclin." J Biol Chem **278**(25): 22877-86.
- He, C. Y., H. H. Ho, et al. (2004). "Golgi duplication in *Trypanosoma brucei*." J Cell Biol **165**(3): 313-21.
- Hirumi, H. and K. Hirumi (1989). "Continuous cultivation of *Trypanosoma brucei* blood stream forms in a medium containing a low concentration of serum protein without feeder cell layers." J Parasitol **75**(6): 985-9.
- Hung, C. H., X. Qiao, et al. (2004). "Clathrin-dependent targeting of receptors to the flagellar pocket of procyclic-form *Trypanosoma brucei*." Eukaryot Cell **3**(4): 1004-14.
- Janetopoulos, C. and P. Devreotes (2006). "Phosphoinositide signaling plays a key role in cytokinesis." J Cell Biol **174**(4): 485-90.
- Kelley, R. J., D. L. Alexander, et al. (1999). "Molecular cloning of p67, a lysosomal membrane glycoprotein from *Trypanosoma brucei*." Mol Biochem Parasitol **98**(1): 17-28.
- Kohl, L., T. Sherwin, et al. (1999). "Assembly of the paraflagellar rod and the flagellum attachment zone complex during the *Trypanosoma brucei* cell cycle." J Eukaryot Microbiol **46**(2): 105-9.
- LaCount, D. J., B. Barrett, et al. (2002). "*Trypanosoma brucei* FLA1 is required for flagellum attachment and cytokinesis." J Biol Chem **277**(20): 17580-8.
- Lagace, T. A., D. M. Byers, et al. (1997). "Altered regulation of cholesterol and cholesteryl ester synthesis in Chinese-hamster ovary cells overexpressing the oxysterol-binding protein is dependent on the pleckstrin homology domain." Biochem J **326** ( Pt 1): 205-13.
- Lee, M. G., B. E. Bihain, et al. (1990). "Characterization of a cDNA encoding a cysteine-rich cell surface protein located in the flagellar pocket of the protozoan *Trypanosoma brucei*." Mol Cell Biol **10**(9): 4506-17.

- Lemmon, M. A. (2003). "Phosphoinositide recognition domains." Traffic **4**(4): 201-13.
- Lester, R. L. and R. C. Dickson (1993). "Sphingolipids with inositolphosphate-containing head groups." Adv Lipid Res **26**: 253-74.
- Levine, T. P. and S. Munro (1998). "The pleckstrin homology domain of oxysterol-binding protein recognises a determinant specific to Golgi membranes." Curr Biol **8**(13): 729-39.
- Levine, T. P. and S. Munro (2002). "Targeting of Golgi-specific pleckstrin homology domains involves both PtdIns 4-kinase-dependent and -independent components." Curr Biol **12**(9): 695-704.
- Li, Z. and C. C. Wang (2003). "A PHO80-like cyclin and a B-type cyclin control the cell cycle of the procyclic form of *Trypanosoma brucei*." J Biol Chem **278**(23): 20652-8.
- Matthews, K. R. (2005). "The developmental cell biology of *Trypanosoma brucei*." J Cell Sci **118**(Pt 2): 283-90.
- Mayor, S. and M. Rao (2004). "Rafts: scale-dependent, active lipid organization at the cell surface." Traffic **5**(4): 231-40.
- McKean, P. G., A. Baines, et al. (2003). "Gamma-tubulin functions in the nucleation of a discrete subset of microtubules in the eukaryotic flagellum." Curr Biol **13**(7): 598-602.
- Minogue, S., J. S. Anderson, et al. (2001). "Cloning of a human type II phosphatidylinositol 4-kinase reveals a novel lipid kinase family." J Biol Chem **276**(20): 16635-40.
- Minogue, S., M. G. Waugh, et al. (2006). "Phosphatidylinositol 4-kinase is required for endosomal trafficking and degradation of the EGF receptor." J Cell Sci **119**(Pt 3): 571-81.
- Mitchell, C. A., R. Gurung, et al. (2002). "Inositol polyphosphate 5-phosphatases: lipid phosphatases with flair." IUBMB Life **53**(1): 25-36.
- Moreira-Leite, F. F., T. Sherwin, et al. (2001). "A trypanosome structure involved in transmitting cytoplasmic information during cell division." Science **294**(5542): 610-2.

- Moreno, S. N., R. Docampo, et al. (1992). "Calcium homeostasis in procyclic and bloodstream forms of *Trypanosoma brucei*. Lack of inositol 1,4,5-trisphosphate-sensitive  $\text{Ca}^{2+}$  release." J Biol Chem **267**(9): 6020-6.
- Nakanishi, S., K. J. Catt, et al. (1995). "A wortmannin-sensitive phosphatidylinositol 4-kinase that regulates hormone-sensitive pools of inositolphospholipids." Proc Natl Acad Sci U S A **92**(12): 5317-21.
- Ngo, H., C. Tschudi, et al. (1998). "Double-stranded RNA induces mRNA degradation in *Trypanosoma brucei*." Proc Natl Acad Sci U S A **95**(25): 14687-92.
- Ogbadoyi, E. O., D. R. Robinson, et al. (2003). "A high-order trans-membrane structural linkage is responsible for mitochondrial genome positioning and segregation by flagellar basal bodies in trypanosomes." Mol Biol Cell **14**(5): 1769-79.
- Oude Weernink, P. A., M. Schmidt, et al. (2004). "Regulation and cellular roles of phosphoinositide 5-kinases." Eur J Pharmacol **500**(1-3): 87-99.
- Overath, P. and M. Engstler (2004). "Endocytosis, membrane recycling and sorting of GPI-anchored proteins: *Trypanosoma brucei* as a model system." Mol Microbiol **53**(3): 735-44.
- Pays, E., L. Vanhamme, et al. (1994). "Genetic controls for the expression of surface antigens in African trypanosomes." Annu Rev Microbiol **48**: 25-52.
- Perry, R. J. and N. D. Ridgway (2006). "Oxysterol-binding protein and vesicle-associated membrane protein-associated protein are required for sterol-dependent activation of the ceramide transport protein." Mol Biol Cell **17**(6): 2604-16.
- Phelan, J. P., S. H. Millson, et al. (2006). "Fab1p and AP-1 are required for trafficking of endogenously ubiquitylated cargoes to the vacuole lumen in *S. cerevisiae*." J Cell Sci **119**(Pt 20): 4225-34.
- Ploubidou, A., D. R. Robinson, et al. (1999). "Evidence for novel cell cycle checkpoints in trypanosomes: kinetoplast segregation and cytokinesis in the absence of mitosis." J Cell Sci **112** ( Pt 24): 4641-50.

- Robinson, D. R., T. Sherwin, et al. (1995). "Microtubule polarity and dynamics in the control of organelle positioning, segregation, and cytokinesis in the trypanosome cell cycle." J Cell Biol **128**(6): 1163-72.
- Salazar, G., B. Craige, et al. (2005). "Phosphatidylinositol-4-kinase type II alpha is a component of adaptor protein-3-derived vesicles." Mol Biol Cell **16**(8): 3692-704.
- Shelton, S. N., B. Barylko, et al. (2003). "Saccharomyces cerevisiae contains a Type II phosphoinositide 4-kinase." Biochem J **371**(Pt 2): 533-40.
- Sherwin, T. and K. Gull (1989). "The cell division cycle of Trypanosoma brucei: timing of event markers and cytoskeletal modulations." Philos Trans R Soc Lond B Biol Sci **323**(1218): 573-88.
- Sherwin, T. and K. Gull (1989). "Visualization of detyrosination along single microtubules reveals novel mechanisms of assembly during cytoskeletal duplication in trypanosomes." Cell **57**(2): 211-21.
- Shi, H., A. Djikeng, et al. (2000). "Genetic interference in Trypanosoma brucei by heritable and inducible double-stranded RNA." Rna **6**(7): 1069-76.
- Stebeck, C. E. and T. W. Pearson (1994). "Major surface glycoproteins of procyclic stage African trypanosomes." Exp Parasitol **78**(4): 432-6.
- Tielens, A. G. and J. J. Van Hellemond (1998). "Differences in energy metabolism between trypanosomatidae." Parasitol Today **14**(7): 265-72.
- Toker, A. (1998). "The synthesis and cellular roles of phosphatidylinositol 4,5-bisphosphate." Curr Opin Cell Biol **10**(2): 254-61.
- Toker, A. (2002). "Phosphoinositides and signal transduction." Cell Mol Life Sci **59**(5): 761-79.
- Toth, B., A. Balla, et al. (2006). "Phosphatidylinositol 4-kinase IIIbeta regulates the transport of ceramide between the endoplasmic reticulum and Golgi." J Biol Chem.
- Troeberg, L., R. N. Pike, et al. (1997). "Production of anti-peptide antibodies against trypanopain-Tb from Trypanosoma brucei: effects of antibodies on enzyme activity against Z-Phe-Arg-AMC." Immunopharmacology **36**(2-3): 295-303.

- Vannier-Santos, M. A., A. Martiny, et al. (1999). "Impairment of sterol biosynthesis leads to phosphorus and calcium accumulation in Leishmania acidocalcisomes." Microbiology **145** ( Pt 11): 3213-20.
- Vickerman, K. and T. M. Preston (1970). "Spindle microtubules in the dividing nuclei of trypanosomes." J Cell Sci **6**(2): 365-83.
- Walch-Solimena, C. and P. Novick (1999). "The yeast phosphatidylinositol-4-OH kinase pik1 regulates secretion at the Golgi." Nat Cell Biol **1**(8): 523-5.
- Wang, Y. J., J. Wang, et al. (2003). "Phosphatidylinositol 4 phosphate regulates targeting of clathrin adaptor AP-1 complexes to the Golgi." Cell **114**(3): 299-310.
- Wang, Z., J. C. Morris, et al. (2000). "Inhibition of Trypanosoma brucei gene expression by RNA interference using an integratable vector with opposing T7 promoters." J Biol Chem **275**(51): 40174-9.
- Wirtz, E. and C. Clayton (1995). "Inducible gene expression in trypanosomes mediated by a prokaryotic repressor." Science **268**(5214): 1179-83.
- Wirtz, E., S. Leal, et al. (1999). "A tightly regulated inducible expression system for conditional gene knock-outs and dominant-negative genetics in Trypanosoma brucei." Mol Biochem Parasitol **99**(1): 89-101.
- Wong, K. and L. C. Cantley (1994). "Cloning and characterization of a human phosphatidylinositol 4-kinase." J Biol Chem **269**(46): 28878-84.
- Wong, K., R. Meyers dd, et al. (1997). "Subcellular locations of phosphatidylinositol 4-kinase isoforms." J Biol Chem **272**(20): 13236-41.
- Woodward, R. and K. Gull (1990). "Timing of nuclear and kinetoplast DNA replication and early morphological events in the cell cycle of Trypanosoma brucei." J Cell Sci **95** ( Pt 1): 49-57.



## **VITAE**

Melissa Jeane Rodgers was born in Tripoli, Libya on December 27, 1969 to Betty and Kirby Rodgers. Melissa grew up in Dallas, Texas and graduated from the Episcopal School of Dallas in 1988. Melissa attended the University of North Texas where she earned a Bachelor of Science degree in Biochemistry in 1993. Melissa lived and worked in Austin, Texas before entering the Graduate Program in Cell Regulation at the University of Texas Southwestern Medical Center at Dallas in 1999. Soon thereafter she joined the lab of Dr. Meg Phillips. She will earn her Ph.D. in Cell Regulation from the University of Texas Southwestern Medical Center at Dallas in December, 2006.

Permanent Address: 4137 Parkside Dr.  
Dallas, Texas 75209